

**NASA  
Technical  
Paper  
2091**

January 1983

# Direct Nuclear-Pumped Lasers

N. W. Jalufka

NASA  
TP  
2091  
c.1

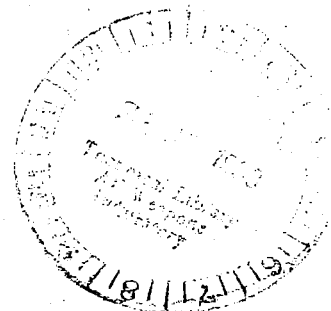
LOAN COPY: RETURN TO  
TECHNICAL LIBRARY.

0134931



TECH LIBRARY KAFB, NM

**NASA**



**NASA  
Technical  
Paper  
2091**

1983

TECH LIBRARY KAFB, NM



0134931

# Direct Nuclear-Pumped Lasers

N. W. Jalufka  
*Langley Research Center  
Hampton, Virginia*

**NASA**  
National Aeronautics  
and Space Administration  
  
Scientific and Technical  
Information Branch



## CONTENTS

INTRODUCTION . . . . .	1
PHYSICS OF NUCLEAR-PUMPED LASERS . . . . .	2
NEUTRON SOURCES . . . . .	7
Thermal Reactors . . . . .	7
Fast-Burst Reactors . . . . .	8
HISTORICAL DEVELOPMENT . . . . .	8
DIRECT NUCLEAR-PUMPED LASERS USING THE $^3\text{He}(n,p)^3\text{H}$ REACTION . . . . .	11
Reactor Experimental Setup . . . . .	11
$^3\text{He}$ -Ar System . . . . .	13
$^3\text{He}$ -Xe System . . . . .	16
$^3\text{He}$ -Kr System . . . . .	20
$^3\text{He}$ -Ne System . . . . .	20
$^3\text{He}$ -Cl System . . . . .	21
$^3\text{He}$ -CO System . . . . .	21
Large-Volume Excitation of $^3\text{He}$ and Noble Gas Systems . . . . .	25
Direct Nuclear-Pumped Oscillator and Amplifier . . . . .	29
Other Systems Investigated . . . . .	30
Summary of $^3\text{He}$ Experiments . . . . .	31
DIRECT NUCLEAR-PUMPED LASERS USING FISSIONABLE WALL COATINGS . . . . .	32
CO System . . . . .	32
$^4\text{He}$ and Noble Gas Systems . . . . .	33
Ne- $\text{N}_2$ System . . . . .	34
He-Hg System . . . . .	35
$^4\text{He}$ -CO and $^4\text{He}$ -CO <sub>2</sub> Systems . . . . .	35
Ar-Xe Multiple-Pass System . . . . .	35
Other Experiments . . . . .	37
$\text{N}_2$ -CO <sub>2</sub> TRANSFER LASER . . . . .	38
DIRECT NUCLEAR-PUMPED LASERS USING $^{235}\text{UF}_6$ . . . . .	39
SYSTEM STUDY . . . . .	40
RELATED THEORY AND EXPERIMENTS . . . . .	41
CONCLUSION . . . . .	43
REFERENCES . . . . .	45



## INTRODUCTION

The concept of a laser powered directly by nuclear energy came into existence shortly after the laser was invented. Scientists were intrigued by the idea of converting the high energy density of the nuclear reactor directly into a laser beam to produce an extremely high-power laser. Initial research to demonstrate such a laser was meager because of limited funding and reactor availability. As an outgrowth of programs to develop the nuclear-powered rocket and gas core nuclear reactor, NASA supported (during the 1970's) a rather broad program of research in direct nuclear-pumped lasers. NASA was interested in the nuclear-pumped laser for several reasons:

1. Direct nuclear-pumped lasers were envisioned as one method of extracting energy from the gas core reactor.
2. One could imagine numerous applications for a space-based high-power laser including laser propulsion, communication, power transmission, area illumination, smog dispersal, and snow removal.
3. There were also numerous terrestrial applications for high-power lasers including nuclear fusion research, photochemistry, and manufacturing processes.
4. A direct nuclear-pumped laser could potentially be a compact, self-contained system requiring a minimum of maintenance, ideal for space application.

The primary objectives of the NASA program were twofold:

1. To demonstrate high power output (1 kW) from a laser powered solely by nuclear energy
2. To investigate the use of gaseous uranium as part of the laser gas mixture in order to determine the feasibility of a self-contained, nuclear-powered reactor-laser system.

The program, structured as broadly as possible within budgetary constraints, was directed toward the ultimate goal of a space-based self-critical nuclear-powered laser with the (gaseous) reactor core and the lasing media contained in a single optical cavity. The program consisted of an in-house effort at Langley Research Center and numerous grants and contracts. One of the first priorities of the program was to establish a data base for plasmas produced by nuclear reaction. It was necessary to determine the dominant atomic and molecular processes characterizing these plasmas in order to determine how one might obtain a population inversion in the lasing gas. Once these processes were determined and experience was gained in carrying out experiments in the radiation environment of a nuclear reactor, the program advanced rapidly. Figure 1 shows the various direct nuclear-pumping reactions that have been employed in the development of direct nuclear-pumped lasers. Figure 1(a) shows the wall coating technique in which a coating of  $^{10}\text{B}$  or a  $^{235}\text{U}$  compound is deposited on the walls of the laser tube. Thermal neutrons from an external source interact with the coatings to produce high-energy particles (fission fragments, alpha particles, or protons) which ionize and excite the lasing gas. Figure 1(b) shows the volumetric pumping concept in which  $^3\text{He}$  or gaseous  $^{235}\text{UF}_6$  is mixed with the lasing gas. Interaction of

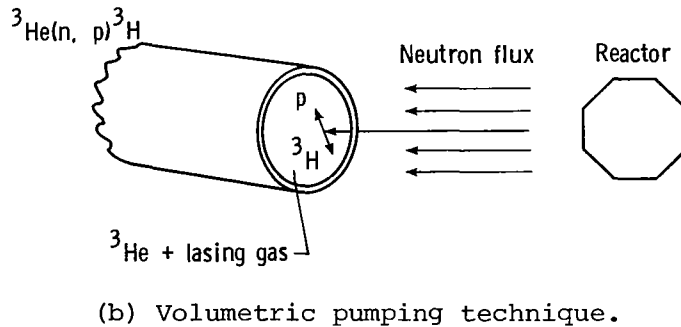
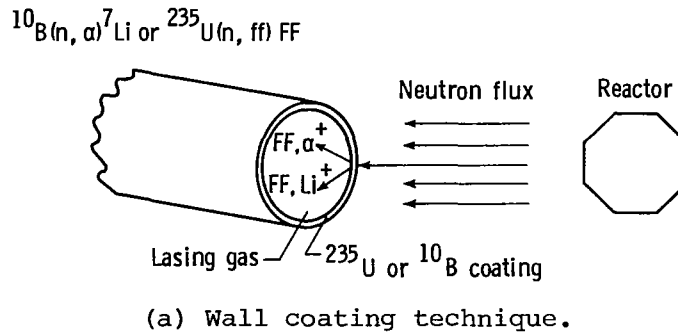


Figure 1.- Direct nuclear-pumping reactions.

these gases with thermal neutrons produce high-energy particles throughout the lasing gas which uniformly ionize and excite the medium. Considerable success was obtained with both approaches.

Research in nuclear-pumped lasers was also supported by the Energy Research and Development Administration (the forerunner of the Department of Energy), the U.S. Army, and Sandia Laboratories. The emphasis in this paper, however, is on the program supported by NASA.

#### PHYSICS OF NUCLEAR-PUMPED LASERS

Rapid development of nuclear-pumped lasers came about only after the expenditure of much effort to understand nuclear-induced plasmas. It was realized at the outset that plasmas produced by direct interaction of nuclear fission products with a lasing gas would be inherently different from plasmas produced by other means. A major characteristic of the fission fragments was their extremely large amount of kinetic energy (of the order of  $10^6$  times that of electrically produced plasmas). Much information about the interactions of energetic heavy particles with gases was available from previous research on radiation effects in the upper atmosphere, on the physics of nuclear detectors, on nuclear ionization enhancement in plasma devices, and on radiation-induced luminescence. Research on ionization chambers had determined the stopping distances of nuclear particles to be of the order of centimeters in gases at pressures of 100 kPa. Therefore a large portion of the kinetic energy of these particles would be absorbed in the laser medium only at high pressures. However, low gas pressures were considered at that time to be more favorable to laser

action. An early conclusion was that nuclear-pumped gas lasers would have to operate at high pressures, and consequently the excitation mechanisms producing a population inversion might differ from those in other laser systems. When a high-energy fission fragment is absorbed in a gas, its kinetic energy is lost by inelastic collisions resulting in ionization and excitation of the medium. The free electrons produced in the first few collisions also have considerable kinetic energy and, as a result, contribute to the ionization and excitation processes. The average energy  $W$  required to produce an ion pair is given by

$$W = \bar{E}_i + \left( \frac{N_x}{N_i} \right) \bar{E}_x + \bar{\epsilon} \quad (1)$$

where

$$\bar{E}_i = 1.06V_i$$

$V_i$  ionization potential of the atom

$\bar{E}_x$  average energy expended in atomic excitation,  $0.85V_i$

$\bar{\epsilon}$  average kinetic energy of subexcitation electrons,  $0.31V_i$

$N_x$  number of atoms excited

$N_i$  number of atoms ionized

The numbers of atoms involved,  $N_x$  and  $N_i$ , are related by

$$N_x = 0.53N_i \quad (2)$$

Since there is no external means of heating the free electrons, thermalization at near room temperature would result. The nuclear-induced plasma was therefore characterized by a reasonably high degree of ionization, considerable excitation, and low temperature.

Several excitation mechanisms were known to produce inversions in gas discharge lasers. These mechanisms included

Resonant excitation-energy transfer

Charge exchange

Penning reactions

Dissociative excitation-energy transfer

Electron impact

Charge neutralization

Line absorption



Molecular photodissociation

Radiative cascade pumping

Collisional-radiative recombination

The problem then remained to determine which of these mechanisms might produce an inversion in the nuclear-induced plasma.

The first detailed analysis of nuclear-pumped gas lasers focused on the role that high-energy fission fragments played in the direct excitation of the upper laser level (refs. 1 through 4). The first investigation to consider in some detail the formation of excited states due to the recombination of thermal electrons and the associated radiative and collisional decay of these states was carried out by Russell (ref. 5). He considered pure Ar excited by fission fragments from a thin uranium coating on the end walls of a cavity. Rate equations were developed describing the atomic ion  $\text{Ar}^+$ , the molecular ion  $\text{Ar}_2^+$ , and the excited atomic states in a gas having a degree of ionization of the order of  $10^{-4}$  and an electron temperature less than 2000 K. These equations were solved for a range of thermal neutral flux  $\phi$  from  $1.8 \times 10^{18}$  to  $3.0 \times 10^{18}$   $\text{n/m}^2\text{-s}$  and electron densities  $N_e$  from  $4 \times 10^{18}$  to  $6 \times 10^{18}$   $\text{electrons/m}^3$ . Russell assumed that the excited atomic states could be formed by (1) recombination of thermal electrons with atomic ions, (2) inelastic collisions between excited atoms and thermal electrons, (3) radiative transitions, (4) direct excitation due to fission fragments and high-energy secondary electrons, and (5) the products of dissociative recombination of diatomic ions. The results of this investigation indicated that a direct nuclear-pumped laser utilizing the 4d-5p transition array in argon was achievable.

Schneider (ref. 6) studied the kinetic processes involved in the interaction of nuclear radiation fission fragments with helium. In particular, this work was directed toward the study of excitation of the atomic helium states by direct impact by fission fragments and impact by high-energy secondary electrons. Experiments (refs. 7 and 8) carried out in a training reactor indicated that direct excitation by fission fragments dominated at low pressures, while excitation by secondary electrons dominated at high pressure. These experiments also indicated that the fission fragment excitation in a gas could not be described with an equilibrium model.

One area that received considerable theoretical attention was the distribution of the free electrons in a radiation-produced plasma. Lo and Miley (ref. 9) studied the problem with an integral balance technique applied to a helium plasma produced in a boron-coated tube. They assumed that at the pressures considered ( $>2.7$  kPa), excitation of the neutral atoms was produced predominantly by secondary electrons being slowed down by collision with the neutral gas (i.e., Coulomb collisions with other electrons and ions were neglected). The ionization fraction was restricted to a value approximately less than  $10^{-5}$  and thermal neutron fluxes were restricted to less than  $10^{18}$   $\text{n/m}^2\text{-s}$ . These investigations showed that the electron energy distribution function decreased rapidly at high energies because of the large rate of energy loss by inelastic collision. The high-energy secondary electrons, however, contributed significantly to the "high-energy tail" of the distribution, so that the function was non-Maxwellian. Values of  $W$  (energy required to produce an ion pair) calculated from this distribution agreed relatively well with measured values.

Hassan and Deese (ref. 10) used a Boltzmann equation formulation to study the electron distribution in a helium plasma produced by fission fragments from a wall coating. This formulation took into account the effects of ambipolar diffusion,

elastic and inelastic collisions, two- and three-body recombination, and ionization. Since the primary electrons generated by the fission fragments were not monoenergetic, the formulation allowed for a source of primary electrons whose distribution was calculated by Guyot et al. (ref. 11). Calculations were carried out for neutron fluxes  $\phi$  from  $3.8 \times 10^{15}$  to  $7.6 \times 10^{18}$  n/m<sup>2</sup>-s, a temperature  $T$  of 300 K, and pressures  $p$  from 13.3 to 100 kPa. Figure 2 shows the calculated distribution function. These calculations showed that a large fraction of the energy of the primary electrons was transferred into excited states.

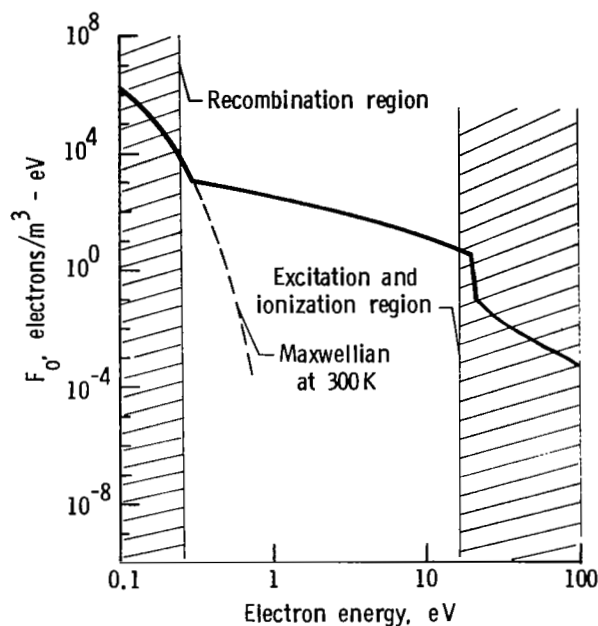


Figure 2.- Calculated electron energy distribution function  $F_0$  in a nuclear-induced He plasma.  $p = 13.3$  kPa;  $T = 300$  K;  $\phi = 10^{20}$  n/m<sup>2</sup>-s.

Deese and Hassan (ref. 12) carried out a detailed study of a nuclear-induced plasma to investigate gain and excited-state populations in the medium. The kinetic model developed in the study treated particles in different quantum states as different species and used the multifluid conservation equations of mass, momentum, and energy to describe the resulting system. The model also took into account ionization, excitation and deexcitation, radiative recombination, spontaneous emission, associative ionization, and dissociative and collisional recombination. Simultaneous effects of electrons and heavy particles in producing the plasma were considered. Calculated values of helium excited-state densities in a plasma produced by wall coatings agreed well with experimental values obtained by Walters (ref. 7). Comparisons were also made with the model developed by Thiess and Miley (ref. 13).

During extensive kinetic modeling of a He-N<sub>2</sub>-CO<sub>2</sub>-UF<sub>6</sub> system, Hassan (ref. 14) considered charge exchange, Penning ionization, recombination, attachment, mutual neutralization, vibrational-vibrational and vibrational-translational energy transfer, and direct electron impact excitation for the various atomic and molecular species involved. The results of this study suggested that dissociation of CO<sub>2</sub> prevented efficient operation of a nuclear-pumped CO<sub>2</sub> laser system based on this combination

of gases. The calculations were based on a thermal neutron flux of  $3 \times 10^{20}$  n/m<sup>2</sup>-s which was representative of fast-burst reactors. A total pressure of 100 kPa and a temperature of 300 K were used in the calculations to be consistent with the Langley experimental investigation.

Wilson et al. (ref. 15) developed a kinetic model to study the  $^3\text{He-Ar}$  direct nuclear-pumped laser. The principal reactions in the model are shown in figure 3. Investigations based on this kinetic model showed the dominant pumping mechanism to be the formation of  $\text{Ar}^+$  ions by charge transfer to  $\text{He}^+$  and Penning ionization of Ar followed by collisional-radiative recombination and radiative cascading into the upper laser level. If the concentration of lasing species became too high,  $\text{Ar}_2^+$  formed. This led to a decrease in laser output as the molecular ion underwent dissociative recombination that preferentially populated the lower laser level.

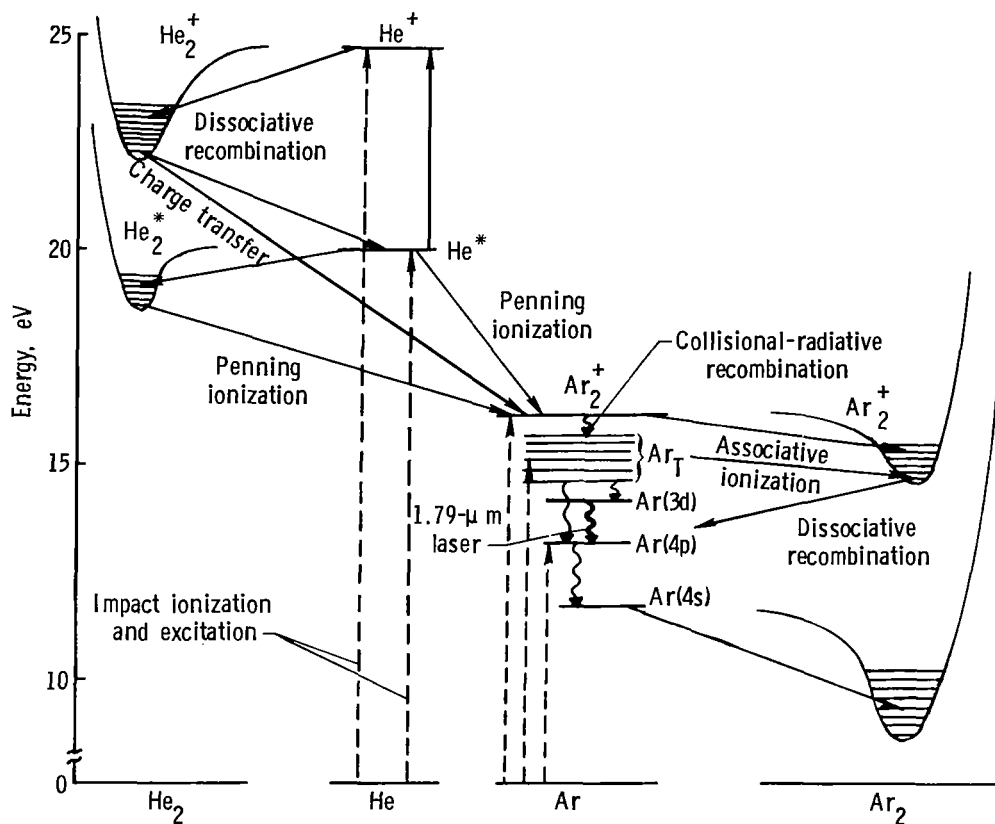


Figure 3.-  $^3\text{He}$ -Ar reactions.

Wilson and De Young (ref. 16) studied the power deposition by neutrons in  $^3\text{He}$  gas. This theoretical study treated in detail the effects of spectral dependence of the neutron flux, neutron attenuation in the  $^3\text{He}$ -filled tube, and transport of the charged particles produced in the  $^3\text{He}(n,p)^3\text{H}$  reaction. An expression for the energy density as a function of position within the tube, tube radius, operating pressure, and neutron fluence was derived. In this investigation, the maximum energy density within the optical cavity was achieved when the tube radius  $a$  (in meters) was given by  $a = 3260/p$  where  $p$  was the operating pressure in pascals. Varying the radius by 50 percent above and below optimum changed the energy density by at most

10 percent, although performance was shown to degrade quickly for radii outside of this range.

Wilson and De Young (ref. 17) studied  $^{235}\text{UF}_6$  as a volumetric energy source with helium as an intermediate energy storage system. They treated neutron attenuation and fission product transport within a laser tube during  $^{235}\text{UF}_6$  pumping of He. Neutron attenuation was found not to be significant for tube sizes and pressure ranges anticipated for laser applications. The investigation showed that maximum power could be deposited in a laser tube when the tube radius was at least as large as the range of the fission fragments. The maximum power was deposited in the helium gas when the tube radius equaled the fission fragment range and the ratio of  $^{235}\text{UF}_6$  partial pressure to total pressure was 0.15, corresponding to a  $^{235}\text{UF}_6$ -He mixing ratio of approximately 1:6.

Although these various investigations added much to the knowledge of kinetic processes in radiation-induced plasmas, they should generally be regarded as a first effort. Because of the high pressures and various gas mixtures employed in nuclear-pumped lasers, many poorly understood reactions take place, although the dominant excitation processes are now known for the  $^3\text{He}$  and noble gas systems. Furthermore, the upper laser level may be populated by a variety of processes depending on the particular laser, so that each laser should be studied in detail to understand the particular processes involved. Consequently, much more research is required to better understand the many processes possible in nuclear-pumped lasers. Until these various processes are understood, scaling of nuclear-pumped lasers to higher efficiency and power will be severely restricted.

## NEUTRON SOURCES

Early theoretical studies (ref. 18) indicated that thermal neutron fluxes up to  $10^{20}$   $\text{n/m}^2\text{-s}$  might be required to reach lasing threshold in a gas laser powered entirely by nuclear reactions. This result precluded the possibility of any source other than a reactor for actual experiments. In fact, many existing reactors (particularly steady-state reactors) did not provide sufficient thermal flux to achieve this threshold. Reactors available to research groups were classified into two categories according to the type of neutrons available to the experiment: thermal reactors and fast-burst reactors.

### Thermal Reactors

Thermal reactors normally provided thermal neutrons for experiments, although fast neutrons were available. These facilities were quite large, since the actual core was surrounded by a moderator (graphite, heavy water, etc.), reflector, and shielding and also required provisions for cooling the core. One particular class of thermal reactors available at several universities, the TRIGA (training, research, isotope production, and general atomic) reactor, provided adequate neutron fluxes for many experiments. Unlike most thermal reactors, the TRIGA reactor could be operated in a pulsed mode, peak fluxes of up to  $5 \times 10^{19}$   $\text{n/m}^2\text{-s}$  being produced in a pulse with full width at half-maximum (FWHM) of 12 ms. The TRIGA had the added advantage of a fairly high repetition rate (about 3 pulses per hour).

The major disadvantage of thermal reactors for nuclear-pumped laser research was having to place the experiment into a beam port for neutron irradiation. This required that all adjustments to the experiment be made remotely because the

experiment was no longer accessible to the researcher once it was placed in the reactor. Furthermore, since the entire experiment was exposed to the thermal flux, activation of the assembly occurred and resulted in long decay times before research personnel could handle the assembly.

### Fast-Burst Reactors

Fast-burst reactors were unshielded and uncooled and, as a result, were very small. They produced peak neutron fluxes up to  $2 \times 10^{21}$  n/m<sup>2</sup>-s in a 200- $\mu$ s (FWHM) pulse. Because of their small size, these reactors were portable and could be placed next to the experiment. After a pulse, they could be removed, so that the experiment was accessible in a relatively short time. Since these reactors produced fast neutrons, it was necessary to use a moderator around the experiment to thermalize the neutrons.

These reactors produced the highest fluxes available and also allowed fairly easy access to the experiment. Their major disadvantage was the long time required for the core to cool, normally about 2 hours after a high-yield pulse, so that the repetition rate was low.

### HISTORICAL DEVELOPMENT

The first comprehensive study of the possibility of powering a gas laser by direct nuclear excitation was carried out in 1964 by Herwig (refs. 1, 18, and 19). Herwig recognized that solid-state lasers were susceptible to radiation damage and also demonstrated that threshold requirements for He-Ne mixtures were theoretically within the reach of some existing reactors. This study also pointed out that a large-diameter He-Ne laser might be possible because of the inherently low electron temperature in the radiation-induced plasma.

After Herwig's study, DeShong in 1965 (ref. 2) carried out more detailed calculations for a He-Ne system. DeShong showed that if a high-pressure large-diameter laser were feasible, direct excitation might be considerably more efficient than a conventional pump cycle. In 1967, DeShong<sup>1</sup> undertook a series of experiments to verify the feasibility of direct nuclear pumping. While his earlier report concentrated on the He-Ne system, these experiments were carried out on a CO<sub>2</sub> laser, most probably because of the much higher efficiency of this system. These experiments showed an initial decrease in the electrical threshold of the laser with increasing thermal neutron flux up to  $5 \times 10^{12}$  n/m<sup>2</sup>-s and then an increase in the threshold until it exceeded the threshold value at zero flux. This occurred at  $2 \times 10^{14}$  n/m<sup>2</sup>-s. DeShong concluded that radiation-induced dissociation of CO<sub>2</sub> was responsible for this reversal at higher fluxes.

During this time period (1966 to 1968), experiments were also in progress by Eerkens et al. (refs. 3, 20, and 21) at Northrop Laboratories using a pulsed TRIGA reactor. This research used <sup>10</sup>B and <sup>235</sup>U coatings and several different gases. Experiments on Ne-O<sub>2</sub> mixtures showed radiation power outputs of 50 W, but no conclusive evidence of lasing. In experiments on noble gases (Ar, Ne, Xe, Kr), strong

---

<sup>1</sup>DeShong, J. A., Jr.: Summary of Model I Nuclear Pumped Gas Laser Experiments. Internal Argonne National Lab. memorandum dated Apr. 29, 1967.

fluorescence was observed, and unusually strong radiation at  $0.6684\text{ }\mu\text{m}$  was observed in Ar. Experiments were also carried out in He-N<sub>2</sub>-CO<sub>2</sub> mixtures with inconclusive results. The studies on the noble gases resulted in some evidence that lasing had been achieved. Although impressive, this evidence was all indirect and was based on the observation that emission at wavelengths that were known to lase in electrical discharges was favored over emission at normally strong fluorescent lines. The emission at the lasing wavelength required a minimum threshold reactor power (although this was not investigated for all the different gases used) and the peak emission was shifted relative to the reactor peak power. These two characteristics would be expected for a lasing system.

Experiments using a TRIGA reactor were also underway during this time period at the University of Illinois (ref. 22). These investigations concentrated on He-Ne mixtures and resulted in a measured gain of up to 15 percent at  $3.39\text{ }\mu\text{m}$ .

Effects of radiation on electrically driven CO<sub>2</sub> lasers were studied by Allario et al. (ref. 23) and Andriakhin et al. (ref. 24). Allario et al. observed a small enhancement in the output of a CO<sub>2</sub> laser when the <sup>4</sup>He was replaced by <sup>3</sup>He and the device was exposed to a thermal neutron flux of less than  $10^{12}\text{ n/m}^2\text{-s}$ . More dramatic was the report by Andriakhin et al. of a twofold to threefold enhancement of the output of an electrically driven CO<sub>2</sub> laser when exposed to a proton beam.

Early experiments using nuclear radiation to power solid-state lasers (refs. 4, 25, and 26) were also carried out. These experiments proved that nuclear radiation would suppress, rather than enhance, lasing action in solids. This phenomenon was not clearly understood, but was generally attributed to effects of radiation damage.

Most major advances in direct nuclear-pumped laser research occurred after 1970 when these systems were better understood. Much of the work prior to 1970 was devoted to studies directed toward nuclear enhancement of electrical lasers with some research into direct nuclear pumping. The results of this early research (up to 1970) are listed in table I. Successful demonstrations of nuclear-pumped lasers in the mid-1970's (refs. 27 through 29) gave increased momentum to nuclear-pumped laser research. Most of this early research was discussed in the review papers by Thom and Schneider (ref. 30). The majority of research after 1970 can be divided into two categories: studies employing <sup>3</sup>He and <sup>235</sup>UF<sub>6</sub> as the excitation method and studies employing <sup>235</sup>U or <sup>10</sup>B coatings on the tube walls for excitation.

At the initiation of the nuclear-pumped laser program at NASA Langley Research Center, the research group was required to make several decisions. These included

1. Which systems should be investigated?
2. What type of reactor would be required for the chosen system?

The research group decided to investigate noble gas lasers using <sup>3</sup>He pumping. This decision was based on the following reasoning:

1. Direct nuclear pumping using a volume excitation source had not yet been demonstrated.
2. Helium is a component of most noble gas lasers; hence it would be straightforward to replace the <sup>4</sup>He with <sup>3</sup>He.

TABLE I.- EXPERIMENTAL STUDIES OF DIRECT PUMPING OF GAS LASERS PRIOR TO 1970

Investigator	Excitation source	Gas	Results
DeShong	Reactor, $^{10}\text{B}$ coating, $\phi \leq 2 \times 10^{14} \text{ n/m}^2\text{-s}$	$\text{CO}_2\text{-N}_2\text{-He}$	Lower electrical threshold flux, $< 5 \times 10^{12} \text{ n/m}^2\text{-s}$ ; threshold larger above $5 \times 10^{13} \text{ n/m}^2\text{-s}$
Andriakhin et al. (ref. 24)	Accelerator, Beam current $< 7 \mu\text{A}$ , 3-MeV protons	$\text{CO}_2\text{-N}_2\text{-He}$	Constant electrical threshold; enhanced output power by a factor of 2 to 3
Allario et al. (ref. 23)	Low-power reactor, $^3\text{He}$ mixture, $\phi < 10^{12} \text{ n/m}^2\text{-s}$	$\text{CO}_2\text{-N}_2\text{-He (Xe)}$	Output enhancement by several percent
Eerkens, DeJuren, et al. (refs. 3, 20, 21)	Pulsed thermal reactor, $^{10}\text{B}$ and $^{235}\text{U}$ coatings, $\phi < 10^{21} \text{ thermal n/m}^2\text{-s}$	$\text{Ne-O}_2$  $\text{Ar, Ne, Kr}$ (plus $\text{O}_2, \text{He}$ ) $\text{CO}_2\text{-N}_2\text{-He}$	Possible lasing; 50-W output with $\approx 1$ -percent efficiency  Strong fluorescence or lasing at $0.6684 \mu\text{m}$ observed in Ar; $\text{O}_2$ ineffective; He increased output somewhat negative
Guyot et al. (ref. 22)	Pulsed fast reactor, $^{10}\text{B}$ coating, $\phi < 10^{19} \text{ thermal n/m}^2\text{-s}$ and fast neutrons	$\text{He-Ne (plus Ar, air)}$	Strong absorption at $3.39 \mu\text{m}$ , but gain observed only with air contamination
	Pulsed thermal reactor, $^{10}\text{B}$ coating, $\phi < 10^{21} \text{ n/m}^2\text{-s}$	$\text{He-Ne, Ne}$	Various measurements of gain and absorption and microwave measurements

- Excitation of gases by nuclear reactions was known to produce mostly ionization, so that electron-ion recombination seemed a likely method of obtaining a population inversion.
- Noble gases, from argon to xenon, had inverted energy levels in many of the known lasing transitions (i.e., the  $n + 1$  level lies lower in energy than the  $n$  level). It appeared therefore that radiative recombination, which scales as  $n^{-3}$  for hydrogenic levels, could lead to a population inversion. This suggested that argon or a heavier noble gas be chosen, since the mechanism would not produce an inversion in a lighter gas such as neon.
- Many continuously operating laser transitions had been observed in noble gases. Consequently, filling the lower laser level would not be a major problem.
- The atomic and molecular processes that might occur in a radiation-induced plasma were known to have short relaxation times, so that even if it were necessary to carry out experiments with a pulsed reactor, it would still be possible to demonstrate continuous lasing so long as the laser output exceeded the various relaxation times of the relevant processes. In the experiments described in this report, the above definition is meant when "continuous lasing" is mentioned.

7. The three nuclear-pumped lasers that had been demonstrated required fairly high neutron fluxes to achieve lasing; hence a fast-burst reactor (with its higher yields) was chosen for the experimental program.

In the following sections, the unique reactor experiments are described and the individual experiments using  $^3\text{He}$  pumping are discussed.

#### DIRECT NUCLEAR-PUMPED LASERS USING THE $^3\text{He}(n,p)^3\text{H}$ REACTION

A class of particularly successful nuclear-pumped lasers, which played a major role in achieving the NASA program goals, was excited by the reaction,



where  $n$  represents the thermal neutron and  $p$  represents the proton.

The use of  $^3\text{He}$  as the fissioning material utilizes the large cross section of  $^3\text{He}$  for thermal neutron capture ( $5.3 \times 10^{-25} \text{ m}^2$ ). It also offered the advantage of being a gas, which readily mixed with a lasing gas to form a homogeneous mixture, so that uniform volume excitation resulted. Furthermore, since many electrically pumped gas lasers used helium (some required it) as a buffer gas, it appeared reasonable to replace the helium in these systems with  $^3\text{He}$  in order to convert an electrical discharge laser to a nuclear-pumped laser. De Young et al. (ref. 31) first attempted to use  $^3\text{He}$  as a fissioning source for a purely nuclear-pumped laser. They used a  $^3\text{He}\text{-Ne-O}_2$  mixture in their laser and a thermal neutron flux of  $2.5 \times 10^{19} \text{ n/m}^2\text{-s}$ . Although lasing was not achieved in this experiment, a gain of approximately 0.9 percent/m at  $0.8446 \text{ }\mu\text{m}$  (OI) was measured. Lasing using  $^3\text{He}$  excitation was successfully demonstrated in 1976 with a  $^3\text{He}\text{-Ar}$  laser (ref. 32).

#### Reactor Experimental Setup

The cross section of a typical volumetric nuclear-pumped laser is illustrated in figure 4. A fast-burst reactor was used as a source of fast neutrons, which were thermalized by the polyethylene moderator. After thermalization, the neutrons were scattered into the laser cell containing a mixture of  $^3\text{He}$  and a lasing gas. The resulting nuclear reactions produced a proton ( $p$ ) and a tritium ion ( $^3\text{H}^+$ ). These ions produced many secondary electrons (by ionizing collisions) which produced further ionization and excitation of the laser medium. These processes led to a population inversion and subsequently to lasing.

A typical experimental setup at the reactor (used by the Langley research team) is shown in figure 5. The polyethylene moderator used in these experiments was normally 0.60 m long with an annular thickness of 0.05 m. The laser cell normally consisted of 0.025-m o.d. quartz tubing about 0.80 m long with Brewster angle windows at each end. For many of the experiments, these windows were of quartz, although other materials such as potassium fluoride (KF), barium chloride ( $\text{BaCl}_2$ ), or sodium chloride ( $\text{NaCl}$ ) were used because of their transmission properties at certain wavelengths. The optical cavity was formed by dielectric-coated mirrors 0.025 m in diameter or, in some cases, by metallic (Ge, Au, Al, Ag) mirrors. These metallic mirrors



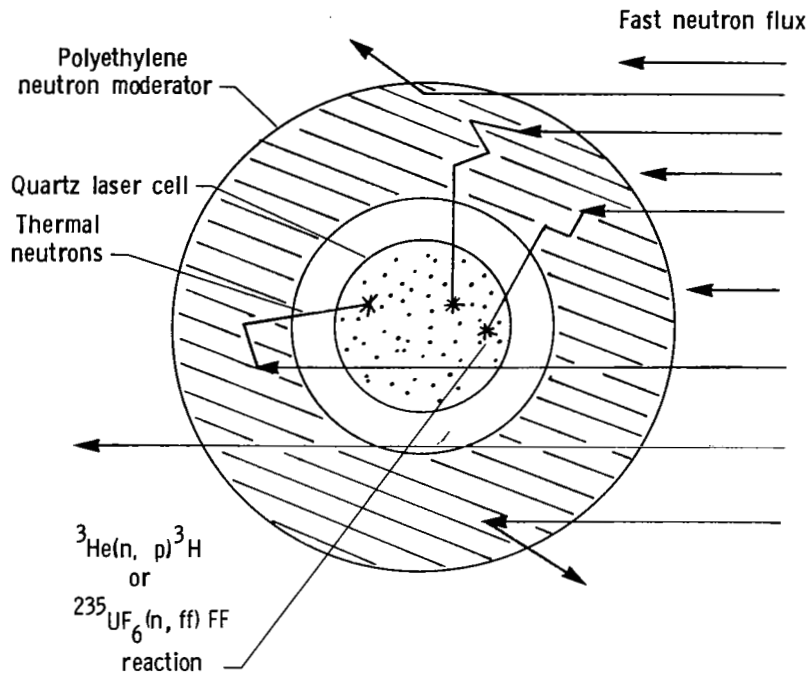


Figure 4.- Cross section of volumetric nuclear-pumped laser.

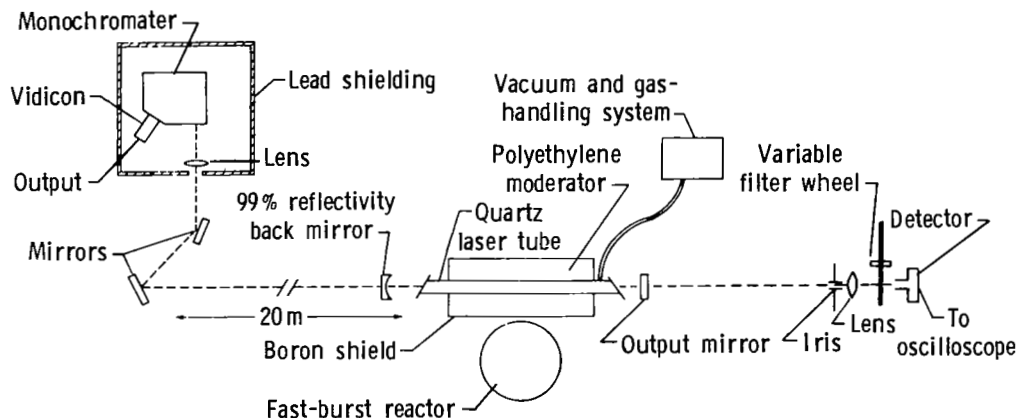


Figure 5.- Experimental arrangement at the reactor.

required a small hole in the output mirror for output coupling of the laser beam. A high vacuum and gas-handling system connected to the laser cell provided the necessary pumping and gas inlet function. Base pressures of the order of 0.133 mPa were attainable with this system. The lasant gas and  $^3\text{He}$  were allowed to mix for 45 to 60 minutes before nuclear excitation.

Electrodes were attached to the laser cell to allow electrical excitation of the gas for alignment of the cavity mirrors and detector. Apertures were mounted in front of the cavity mirrors to ensure that lasing occurred only along the cell centerline.

The fast-burst reactor used by the Langley team in these experiments was located at the U.S. Army Pulse Radiation Facility at Aberdeen Proving Grounds, Maryland. This reactor was typical of the Godiva class, fast-burst reactors used by other research groups. This reactor could produce a neutron flux of  $1.5 \times 10^{21}$  n/m<sup>2</sup>-s inside of the polyethylene moderator. The reactor produced a fast neutron pulse of 50  $\mu$ s (FWHM) which was lengthened to about 200  $\mu$ s (FWHM) after thermalization. Normally, five high yield pulses ( $\approx 10^{21}$  n/m<sup>2</sup>-s) were obtained in a day; for lower yield pulses ( $\approx 10^{19}$  n/m<sup>2</sup>-s), this was increased to about 10 pulses per day. The thermal neutron flux inside the moderator was measured by a self-powered cobalt detector. This detector was 0.60 m long and produced a signal that was proportional to the average thermal neutron flux along the 0.60-m length of the moderator. This detector was experimentally found to be insensitive to the  $\gamma$ -ray and fast neutron irradiation.

A variety of laser detectors were used in these experiments because several wavelength ranges were investigated. In the wavelength range from 1.2  $\mu$ m to 3.8  $\mu$ m, InAs detectors were employed. These varied from single-element to 13-element arrays in a cross configuration which were used to obtain the intensity distribution in the laser beam. In the range from 1.5  $\mu$ m to 6.0  $\mu$ m, a single-element InSb detector cooled to 77 K was used, and beyond 6.0  $\mu$ m, a GeAu detector cooled to 77 K was used. Both the InAs and the InSb detectors were relatively insensitive to the  $\gamma$ -ray and fast neutron flux and could be placed as close as 2 m from the reactor. On the other hand, the GeAu detector was extremely sensitive to the  $\gamma$ -ray and fast neutron fields and could be used only if it was well shielded and placed in a concert maze about 30 m from the reactor. This arrangement required two mirrors to direct the laser beam to the detector. The detector signals were recorded on oscilloscopes. The InAs and InSb detectors were calibrated with a He-Ne laser at 3.39  $\mu$ m.

The visible portion of the emission was transmitted through the back mirror (when the dielectric mirrors were used in the optical cavity) and was focused on the entrance slit of a 0.3-m monochromator equipped with a vidicon optical multichannel analyzer. The optical multichannel analyzer output was fed into a desk-top computer where the spectral data were stored on tape and plotted. Data on lasing and optical emission were obtained simultaneously during each reactor pulse.

### <sup>3</sup>He-Ar System

Lasing was observed from the <sup>3</sup>He-Ar system at two different wavelengths, 1.79  $\mu$ m (ArI,  $3d[1/2]_1^0 - 4p[3/2]_2$  or  $3d[1/2]_0^0 - 4p[3/2]_1$ ) and 1.27  $\mu$ m (ArI,  $3d'[3/2]_1^0 - 4p'[1/2]_1$ ) (ref. 32). Figure 6 shows a typical oscilloscope recording of the laser output. Fast neutrons from the fast-burst reactor were moderated by the polyethylene moderator, which broadened the pulse shape to that shown in the middle trace. The thermal neutrons produce <sup>3</sup>He(n,p)<sup>3</sup>H reactions in the laser cell which by ionizing and exciting the gas produce a population inversion and subsequent lasing in Ar. The laser output is shown in the bottom trace of figure 6. Lasing was initiated with a sharp threshold, a characteristic of all gas lasers, and laser output continued to follow the thermal neutron pulse rather than the fast neutron pulse, demonstrating that it was actually the thermal neutrons which were responsible for pumping the laser. The duration of laser output was long compared with the relaxation time of the various atomic and molecular processes occurring in the gas, and therefore the laser can be considered steady state.

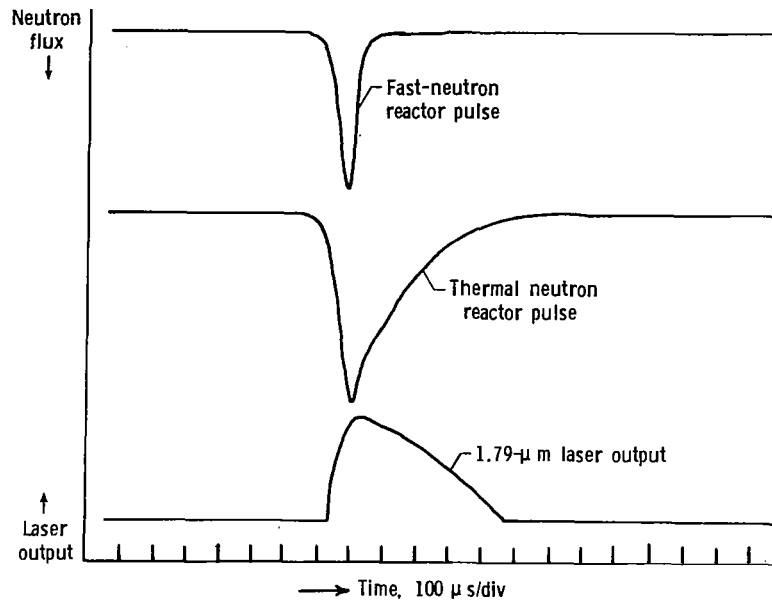


Figure 6.- Oscilloscope recording of  $^3\text{He}$ -Ar laser output.

In figure 7, the laser output at 1.79  $\mu\text{m}$  (ArI) is shown as a function of total  $^3\text{He}$ -Ar pressure for a fixed 1-percent Ar concentration and a thermal neutron flux of  $10^{21} \text{ n/m}^2\text{-s}$ . The laser cavity consisted of two dielectric mirrors, each having a transmission of 1 percent at 1.7  $\mu\text{m}$ . Laser output continued to increase with total pressure up to approximately 200 kPa above which lasing output tended to saturate even though increasing power was deposited in the gas. The exact cause of this saturation was not understood, but was thought to be due to plasma effects such as pressure broadening of the laser energy levels and collisional deactivation of the upper laser level. The solid curve shows the calculated power deposition in the laser cavity volume. At 200 kPa, the peak laser output was 4 W and the power deposited in the volume was 3.8 kW, giving an efficiency of 0.1 percent.

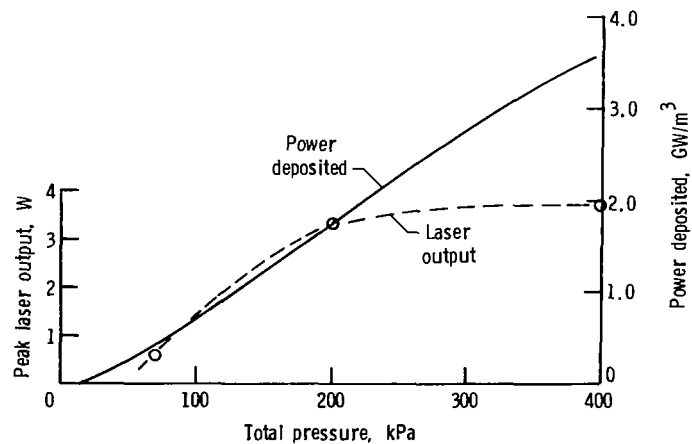


Figure 7.-  $^3\text{He}$ -Ar laser output at 1.79  $\mu\text{m}$  versus total pressure.  
1 percent Ar;  $\phi = 10^{21} \text{ n/m}^2\text{-s}$ .

An argon concentration study was carried out to determine the optimum lasing concentrations. These results (shown in fig. 8) are compared with the calculated  $\text{Ar}^+$  concentration of Wilson et al. (ref. 15) and indicate that the optimum argon concentration for peak power output is near 1 percent.

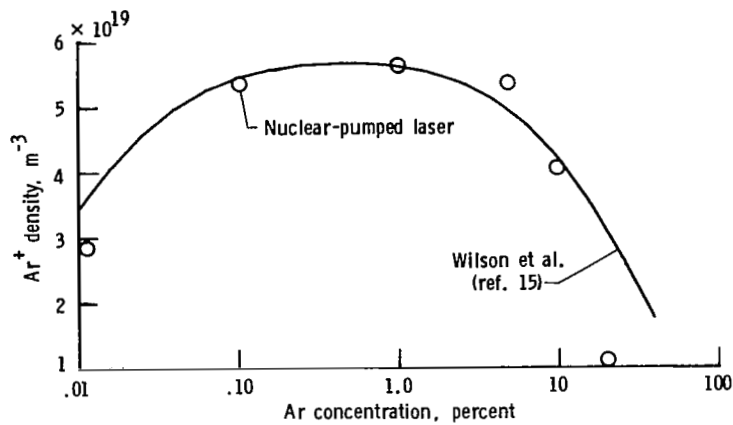


Figure 8.-  $^3\text{He}$ -Ar laser output at  $1.79 \mu\text{m}$  versus Ar concentration.  
 $p = 53 \text{ kPa}$ ;  $\phi = 6 \times 10^{20} \text{ n/m}^2\text{-s}$ .

The scaling of laser output with thermal neutron flux is shown in figure 9. For this study, the total pressure of  $^3\text{He}$ -Ar was held at 80 kPa and the argon concentration at 1 percent. The lasing threshold was found to be  $2.5 \times 10^{20} \text{ n/m}^2\text{-s}$  and the laser output continued to increase linearly with increasing neutron flux. At flux levels higher than those shown in the figure, the laser output was expected to be directly proportional to the thermal neutron flux.

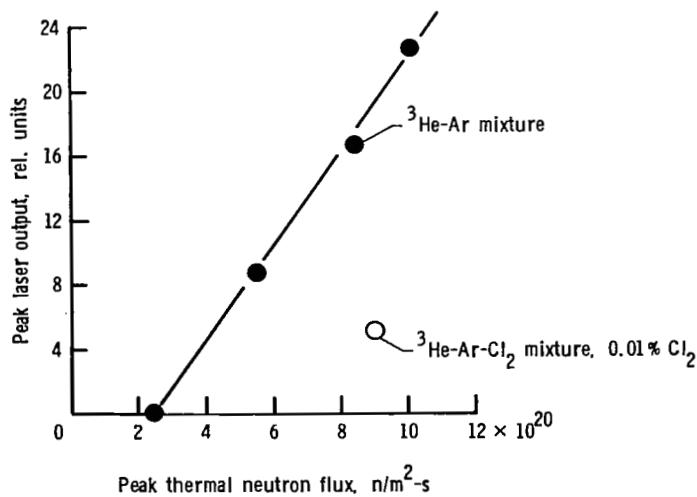


Figure 9.-  $^3\text{He}$ -Ar laser output versus thermal neutron flux. 1 percent Ar;  $p = 80 \text{ kPa}$ .

A small amount of  $\text{Cl}_2$  ( $10^{-2}$  percent) was added to the  $^3\text{He}$ -Ar at 80 kPa to determine its effect on the system. In electrically pumped  $^4\text{He}$ -Ar lasers,  $\text{Cl}_2$ , by effectively depopulating the lower laser level, increases output. For the nuclear-pumped system, however, the laser output decreased as shown in figure 9.

The  $^3\text{He}$ -Ar laser was the first demonstration of a nuclear-powered laser using  $^3\text{He}$  volumetric pumping. The experimental results confirmed the early belief that recombination lasers were likely candidates for nuclear-pumped studies.

### $^3\text{He}$ -Xe System

Direct nuclear pumping of  $^3\text{He}$ -Xe was achieved on four different Xe lines:

$2.026\text{ }\mu\text{m}$  ( $5d[3/2]_1^0 - 6p[3/2]_1$ ),  $3.508\text{ }\mu\text{m}$  ( $5d[7/2]_3^0 - 6p[5/2]_2$ ),  $3.652\text{ }\mu\text{m}$  ( $7p[1/2]_1 - 7s[3/2]_2^0$ ), and  $2.63\text{ }\mu\text{m}$  ( $5d[5/2]_2^0 - 6p[5/2]_2$ ) (refs. 33 and 34).

Although these lines all exhibited similar characteristics, the first three produced low power output ( $<10\text{ W}$ ), while the fourth produced in excess of  $200\text{ W}$ . Lasing at  $2.63\text{ }\mu\text{m}$  could be obtained only with dielectric mirrors having a narrow bandwidth because of competing effects from other lasing transitions in the same array. The other transitions would lase with either dielectric or broadband metallic (Au or Ag) mirrors. Figure 10 is a typical oscilloscope photograph of the output of the direct nuclear-pumped  $^3\text{He}$ -Xe laser. Its behavior was the same as that observed for the  $^3\text{He}$ -Ar laser in that the lasing exhibited a sharp threshold and laser output followed the thermal neutron pulse. The laser output lasted typically 200 to  $400\text{ }\mu\text{s}$  (FWHM), and since this time was long compared with the relaxation time for the relevant atomic and molecular processes, the laser can also be considered a steady-state system.

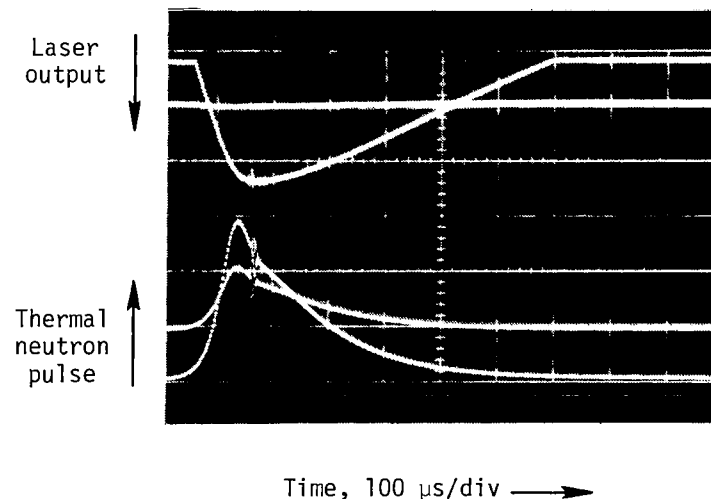


Figure 10.- Oscilloscope photograph of  $^3\text{He}$ -Xe laser output at  $2.03\text{ }\mu\text{m}$ .

In figure 11, the  $^3\text{He-Xe}$  laser output at  $2.63\text{ }\mu\text{m}$  is shown as a function of total pressure. The behavior of the  $2.026\text{-}\mu\text{m}$ ,  $3.508\text{-}\mu\text{m}$ , and  $3.652\text{-}\mu\text{m}$  lines was the same as that observed for the  $^3\text{He-Ar}$  laser, with laser output saturating with increasing pressure above 200 kPa. The  $2.63\text{-}\mu\text{m}$  line, however, increased linearly in power output up to 300 kPa. Voinov et al. (refs. 35 and 36) investigated the  $2.63\text{-}\mu\text{m}$  line by using uranous-uranic oxide coatings for excitation and found nearly linear energy output with pressures up to 400 kPa. Several methods to increase the laser output were attempted, including cavity optimization by varying the output window transmission and the addition of argon. Argon has been shown to be beneficial (ref. 37) in increasing the output (by up to an order of magnitude) of electrically excited He-Xe lasers. During the electrical discharge, the dimer  $\text{Ar}_2$  forms very rapidly. A near resonance between the metastable molecule ( $\text{Ar}_2^*$ ) and the upper laser level of the  $2.026\text{-}\mu\text{m}$  line ( $5d[3/2]_1^0$ ) allows additional pumping of the upper laser level. This was also found to occur for nuclear-excited plasmas, but only at low pressures ( $<80\text{ kPa}$ ). At higher pressures, the laser output decreased with increasing pressure for a fixed concentration of 20 percent argon. This effect was also investigated for the  $2.63\text{-}\mu\text{m}$  line, but the addition of small amounts of argon was found to be detrimental to that system.

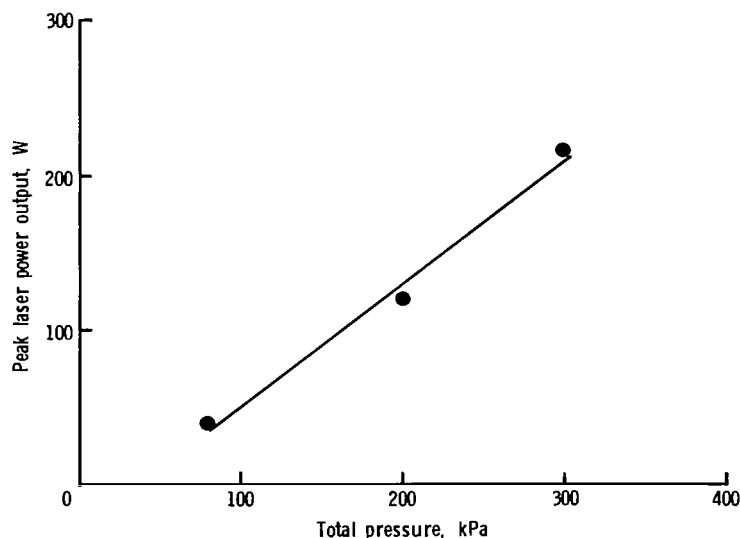


Figure 11.-  $^3\text{He-Xe}$  laser output at  $2.63\text{ }\mu\text{m}$  versus total pressure.

The variation of the  $2.026\text{-}\mu\text{m}$  laser output with peak thermal neutron flux is shown in figure 12. Data were obtained at two different total pressures (53 and 80 kPa). At both pressures, the xenon concentration was 1 percent. The peak laser output was directly proportional to the thermal neutron flux over the range investigated. The lasing threshold was approximately  $4.0 \times 10^{19}\text{ n/m}^2\text{-s}$ , which was the lowest threshold measured for any of the  $^3\text{He}$  and noble gas systems. The thermal flux lasing threshold for the  $2.63\text{-}\mu\text{m}$  line was, however,  $3 \times 10^{20}\text{ n/m}^2\text{-s}$ .

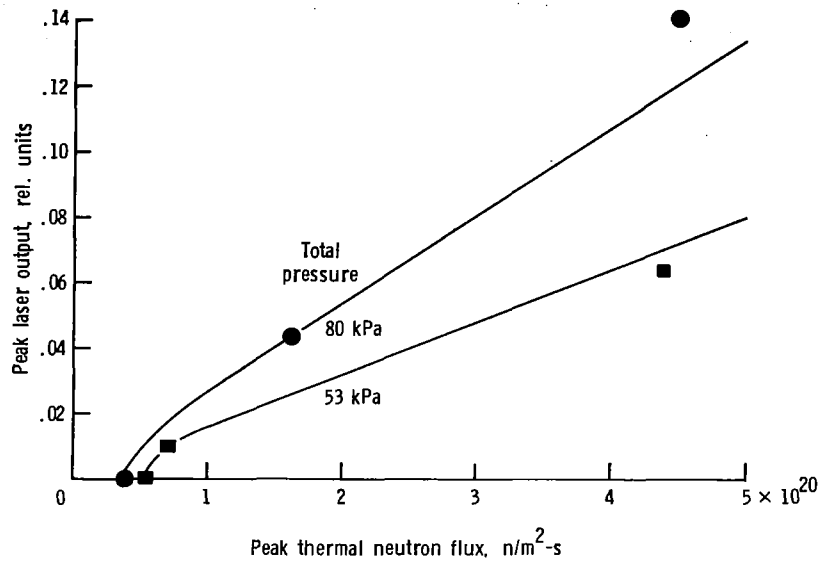


Figure 12.-  $^3\text{He-Xe}$  laser output at  $2.03\ \mu\text{m}$  versus thermal neutron flux. 1 percent Xe.

A concentration study of various XeI laser lines was carried out, with the results shown in figure 13. Optimum Xe concentration was found to vary depending on the lasing wavelength (i.e., transition). Similar studies have been carried out at Los Alamos Scientific Laboratory (ref. 38), and their results are also shown in figure 13. The Los Alamos results for the optimum concentration of Xe differ by an order of magnitude from those of the NASA Langley group. This discrepancy was not completely understood, but may have been due to nonuniform gas mixing.

The gain of the  $^3\text{He-Xe}$  ( $2.026\ \mu\text{m}$ ) laser was measured for a constant Xe concentration of 0.5 percent, a pressure of 100 kPa, and a peak thermal flux of  $3.23 \times 10^{20}\ \text{n/m}^2\text{-s}$ . The results are shown in figure 14 where the round-trip cavity loss (in percent) is plotted as a function of the laser thermal neutron flux threshold. Calibrated neutral density filters were added to the cavity to increase the cavity loss in a stepwise fashion. With no additional cavity loss added, the losses from the Brewster windows and laser mirrors were about 3 percent. Addition of neutral density filters increased the cavity loss and consequently the lasing thermal neutron flux until a cavity loss of 80 percent was reached. At this point, the thermal neutron flux lasing threshold was near the peak flux (no lasing occurred); therefore, the round-trip gain in the cavity was just equal to the round-trip cavity loss and may be calculated from

$$\beta = \frac{1}{2L} \ln \frac{1}{T^2 R_1 R_2} \quad (3)$$

where  $\beta$  is the threshold gain per unit length,  $L$  is the gain length of the laser,  $T$  is the transmission of the neutral density filters, and  $R_1$  and  $R_2$  are the mirror reflectivities. In this manner, a gain of 200 percent/m was determined for this transition. This reasonably high gain explained in part why this particular transition had such a low thermal neutron flux lasing threshold.

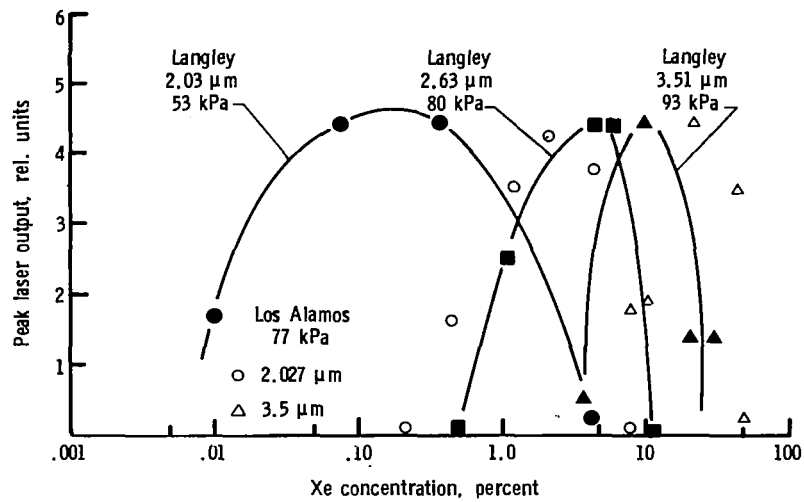


Figure 13.-  $^3\text{He}$ -Xe laser output versus Xe concentration.

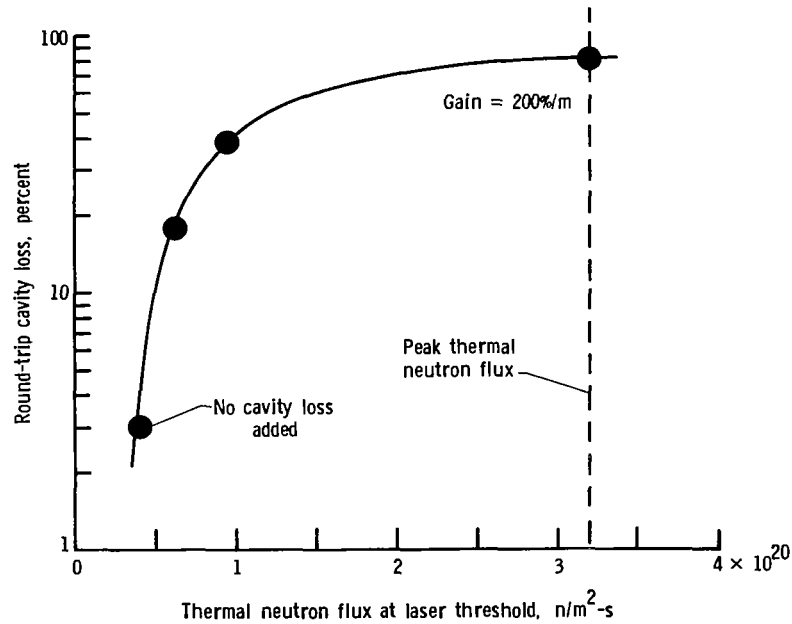


Figure 14.- Gain of  $^3\text{He}$ -Xe laser at 2.03  $\mu\text{m}$ . Gain length = 0.40 m; 0.5 percent Xe;  $p = 100 \text{ kPa}$ .

The  $^3\text{He}$ -Xe laser could be operated on several different lasing transitions, most of which resulted from recombination. The 2.03- $\mu\text{m}$  line had the lowest thermal neutron flux threshold of these transitions; consequently, it was studied in more detail since its low threshold allowed more reactor pulses per day.



### $^3\text{He-Kr}$ System

Figure 15 shows the output of the  $^3\text{He-Kr}$  direct nuclear-pumped laser at a Kr concentration of 0.5 percent, a total pressure of 50 kPa, and a peak thermal neutron flux of  $1.55 \times 10^{21} \text{ n/m}^2\text{-s}$  (ref. 19). Lasing wavelengths at  $2.52 \mu\text{m}$  and  $2.19 \mu\text{m}$  were determined with a variable filter. The laser output at  $2.19 \mu\text{m}$  ( $4d[3/2]_2^0 - 5p[3/2]_2$ ) was considerably less than that at  $2.52 \mu\text{m}$  ( $4d[1/2]_1^0 - 5p[3/2]_1$ ). Peak laser output was 1 mW at 26.6 kPa. The cavity for these measurements consisted of two 2-m radius of curvature mirrors, each having a reflectivity of 95 percent at  $2.5 \mu\text{m}$ . The mirror separation was 0.80 m. The Kr concentration (0.5 percent) should have been near optimum as determined from electrically pulsed afterglow experiments. The observed high thermal neutron flux lasing threshold of  $1.1 \times 10^{21} \text{ n/m}^2\text{-s}$  was probably due to both laser transitions terminating in the same lower level. Both transitions lased simultaneously because of the broad bandwidth of the dielectric mirrors. This system is also a recombination laser, but its high lasing threshold along with its low power output precluded any extensive study.

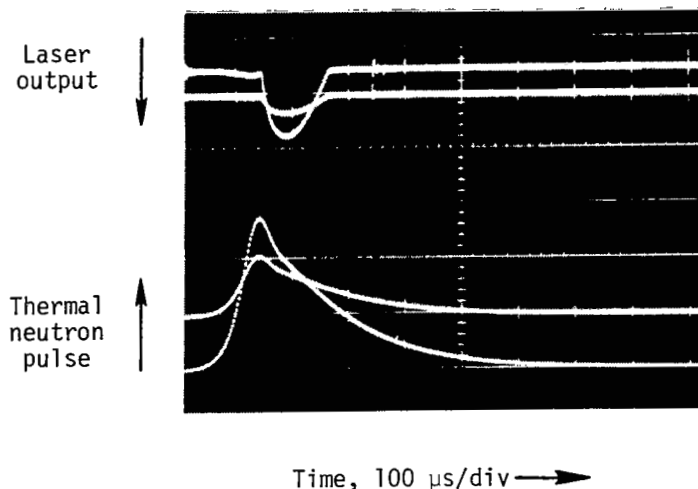


Figure 15.- Oscilloscope photograph of  $^3\text{He-Kr}$  laser output.

### $^3\text{He-Ne}$ System

Carter et al. (ref. 39) have carried out experiments on direct nuclear pumping of  $^3\text{He-Ne}$  systems using the heavy water reactor at Georgia Institute of Technology as well as an Argonaut reactor at the University of Florida. The heavy water reactor was used for experiments with a thermal neutron flux range from  $10^{13}$  to  $10^{18} \text{ n/m}^2\text{-s}$ . The Argonaut was used for experiments at flux levels from  $2 \times 10^9$  to  $2 \times 10^{16} \text{ n/m}^2\text{-s}$ . Both reactors were operated in a continuous mode.

Gain in a mixture of  $^3\text{He-Ne}$  (5:1) at a total pressure of 40 kPa was measured with a 0.5-mW He-Ne oscillator at  $0.6328 \mu\text{m}$ . A maximum amplification of 770 percent/m was measured at a thermal neutron flux of  $2 \times 10^{16} \text{ n/m}^2\text{-s}$ . Experiments to demonstrate continuous-wave (CW) lasing of the nuclear-pumped  $^3\text{He-Ne}$  laser were carried out at a total pressure of 40 kPa, and a ratio of stimulated to spontaneous emission of approximately 60 was determined. The thermal neutron flux lasing threshold was  $2 \times 10^{15} \text{ n/m}^2\text{-s}$ . Peak laser output was only a few microwatts.

This system represented another major step in direct nuclear pumping in that it was the first steady-state (continuous) laser and was not a recombination laser. The laser most probably operates by energy transfer from the helium  $2^1S_0$  metastable state to the neon upper laser level  $(5s'[1/2]_1^0)$ .

### $^3\text{He}\text{-Cl}$ System

Lasing at  $1.587\ \mu\text{m}$  ( $3d^4F_{9/2} - 4p^4D_{7/2}$ ) was achieved in a mixture of 0.008 percent Cl and 99.002 percent  $^3\text{He}$  at a total pressure of 80 kPa (ref. 40). The thermal neutron flux lasing threshold was  $7 \times 10^{19}\ \text{n/m}^2\text{-s}$ . The laser cavity consisted of two 2-m radius of curvature mirrors dielectric coated for maximum reflectivity (98.4 percent) at  $1.7\ \mu\text{m}$ . The maximum laser output power was about 0.1 W. Increasing the Cl concentration to 0.17 percent terminated the lasing action. This system operated at significantly lower concentrations than the Ar, Xe, or Kr nuclear-pumped lasers. This behavior was thought to be due to the formation of  $\text{Cl}^-$  at the higher concentration which reduced the electron density and thus the recombination rate.

### $^3\text{He}\text{-CO}$ System

Direct nuclear pumping of  $^3\text{He}$  and noble gas lasers demonstrated the feasibility of using  $^3\text{He}$  as a volumetric source of excitation. These lasers, since they were mostly recombination lasers, were not the most likely candidates for efficient high-power nuclear lasers. This was apparent at the outset because the low quantum efficiency of recombination lasers was a limiting factor. The most efficient lasers in operation were the  $\text{CO}_2$  and CO molecular lasers. Nuclear-pumped lasing in CO had been demonstrated (ref. 27), but not with  $^3\text{He}$  pumping. Considerable research was carried out on both of these systems. Only the CO laser, however, was successfully pumped directly by a nuclear reactor.

The high power output and high extraction efficiency of the CO laser made it an interesting candidate for nuclear pumping. Consequently, a considerable amount of research was carried out on this system. Multiline lasing on the CO molecule at approximately  $5\ \mu\text{m}$  was achieved in a laser tube assembly cooled by liquid nitrogen (ref. 41). The laser tube was constructed of 0.025-m i.d. quartz tubing with the ends cut at the Brewster angle. The central 0.60 m of the tube was wrapped with 0.007-m o.d. polyvinylchloride tubing through which liquid nitrogen flowed. With this arrangement, a tube wall temperature of 100 K ( $\pm 5\ \text{K}$ ) could be maintained, and a gas temperature of approximately 150 K was calculated from the thermodynamic variables. The laser cavity consisted of a 10-m radius of curvature, gold-coated mirror and a flat gold-coated mirror, each having a diameter of 0.025 m. Output coupling was through a 0.002-m-diameter hole in the flat mirror. The cavity was aligned by using a CW He-Ne laser lasing at  $0.6328\ \mu\text{m}$ . The experimental arrangement is shown in figure 16. With an InSb detector, placed 6 m from the output mirror, no appreciable noise pickup during the reactor pulse was observed. Wavelength discrimination was achieved with broadband interference filters.

The laser output and the thermal neutron flux in the moderator are shown as functions of time in figure 17. The laser output showed a sharp thermal flux threshold at  $3 \times 10^{20}\ \text{n/m}^2\text{-s}$  and started to decrease before the flux peaked. This behavior was in contrast to the  $^3\text{He}$  and noble gas systems for which the laser output followed the thermal neutron flux. The decrease in the laser output before peak flux was reached was most probably due to heating of the laser gas resulting in a reduction

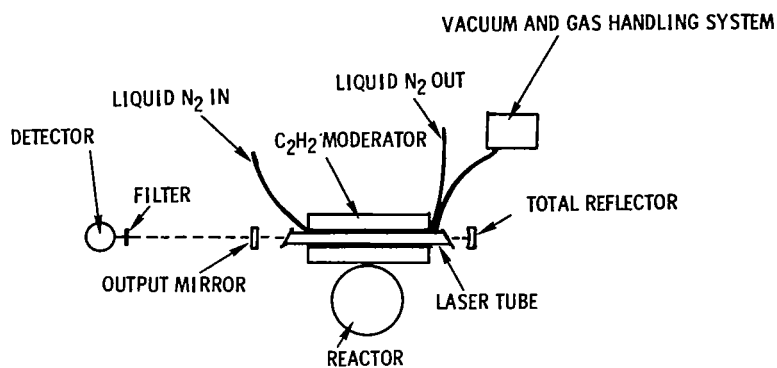


Figure 16.- Experimental arrangement of  $^3\text{He}$ -CO laser.

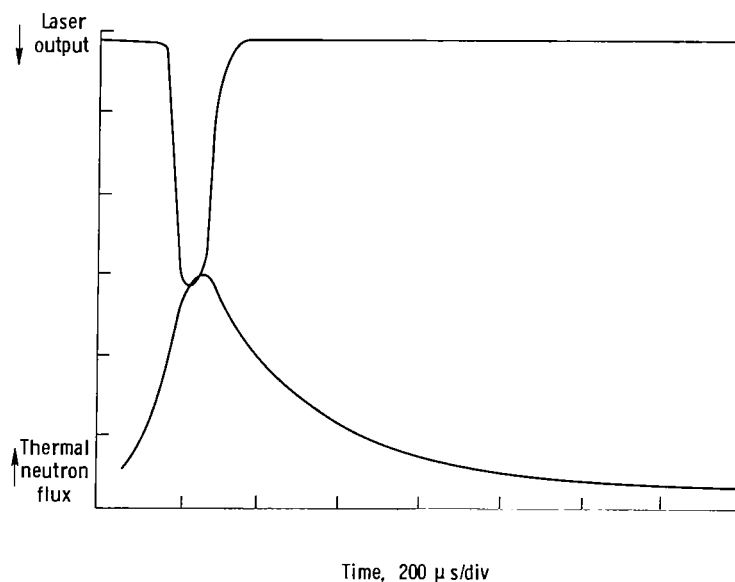


Figure 17.- Oscilloscope recording of  $^3\text{He}$ -CO laser output.

of the vibrational-vibrational transfer rate for the CO molecules and a corresponding increase in the vibrational-translational rate.

The laser output at a total pressure of 180 kPa is shown in figure 18 plotted versus CO concentration. Peak laser output was obtained at a CO concentration of 5 percent.

The beneficial effects of  $\text{N}_2$  on electrically pumped CO lasers were well known. The vibrational levels of  $\text{N}_2$  are nearly resonant with those of CO, so that the energy deposited in  $\text{N}_2$  is transferred to CO without excessive loss. Excitation of the electrically pumped CO laser was due to electron impact, whereas excitation of the nuclear-pumped laser was probably due to recombination of the dimer ion ( $\text{C}_2\text{O}_2^+$ ) and transfer of energy from the  $\text{CO}(a^3\Pi)$  metastable state. It was not apparent, therefore, that the addition of  $\text{N}_2$  to the nuclear-pumped CO laser would be beneficial. Figure 19 shows the CO laser output as a function of  $\text{N}_2$  concentration for a system containing 5 percent CO at a total pressure of 80 kPa.  $\text{N}_2$  was beneficial when added in an amount equal to the CO concentration.

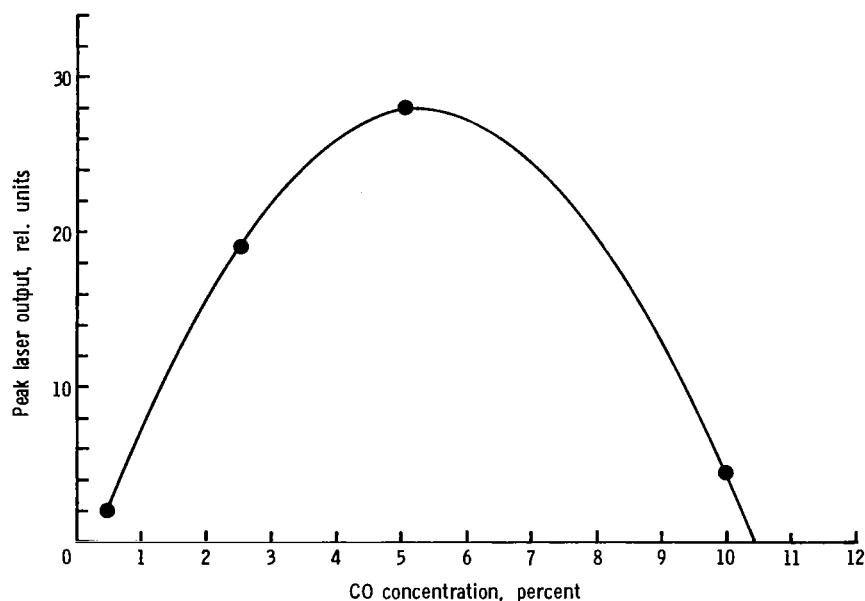


Figure 18.-  $^3\text{He}$ -CO laser output versus CO concentration.  
 $p = 180 \text{ kPa}$ .

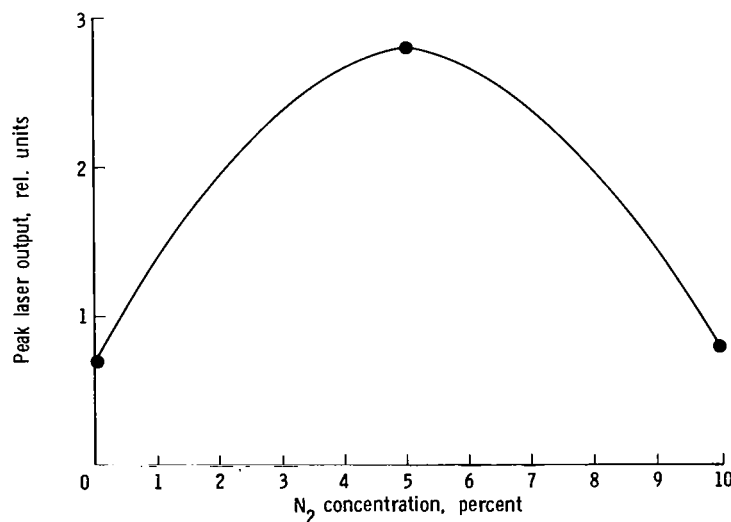


Figure 19.-  $^3\text{He}$ -CO laser output versus  $\text{N}_2$  concentration.  
 5 percent CO;  $p = 80 \text{ kPa}$ .

Scaling of the laser output with total pressure up to 300 kPa is shown in figure 20. Peak power output was obtained at a total pressure of about 200 kPa. Increasing the total pressure to 300 kPa decreased laser output. This pressure should have been near optimum for energy deposition in the 0.0125-m-radius tube (ref. 16). The laser output probably decreased because of depletion of the  $\text{C}_2\text{O}_2^+$  molecular ion by the formation of higher order cluster ions (ref. 41).

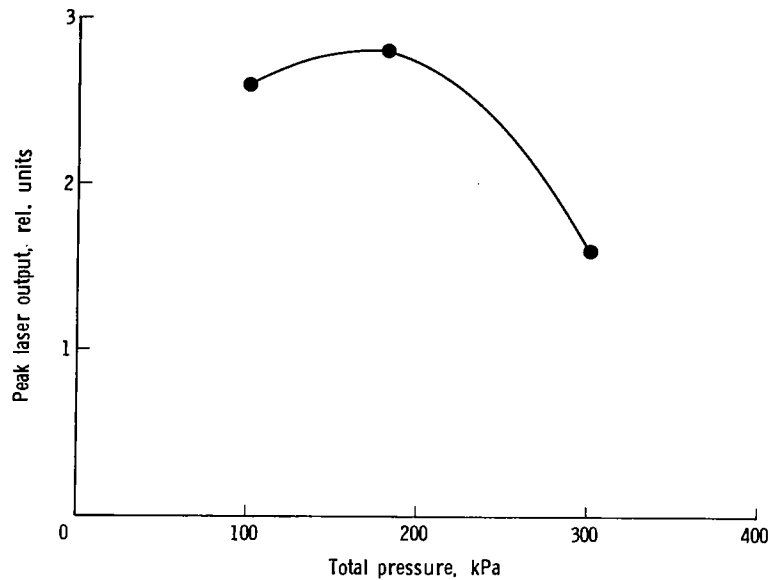


Figure 20.-  $^3\text{He}$ -CO laser output versus total pressure.  
 $\phi = 10^{21} \text{ n/m}^2\text{-s}$ .

Scaling of the laser output with thermal neutron flux is shown in figure 21. These results were obtained at a total pressure of 80 kPa (5 percent CO and 5 percent  $\text{N}_2$ ). The behavior of the  $^3\text{He}$ -CO laser differed from that of  $^3\text{He}$  and noble gas systems: the  $^3\text{He}$ -CO laser output scaled more nearly with the square of the thermal neutron flux whereas  $^3\text{He}$  and noble gas systems exhibited first-order behavior.

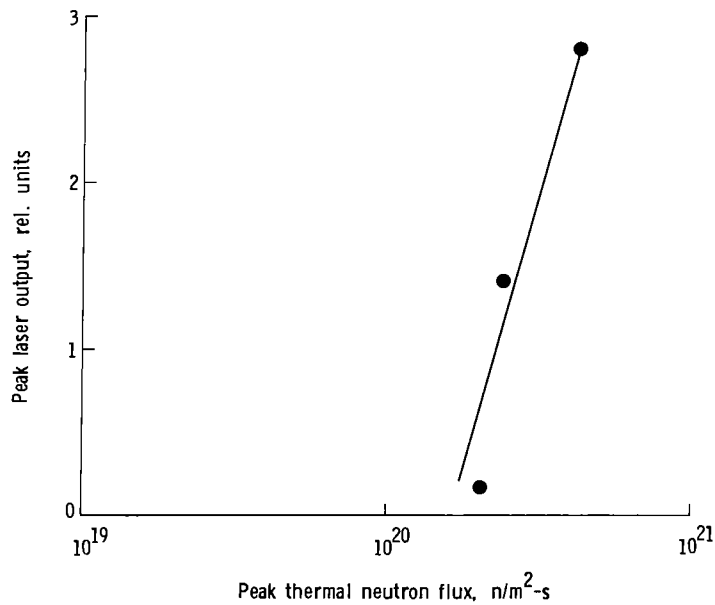


Figure 21.-  $^3\text{He}$ -CO laser output versus thermal neutron flux.  
 $p = 80 \text{ kPa}$ .

A single-element detector ( $10^{-6} \text{ m}^2$ ) was used to detect the laser signal. Consequently, it was not possible to determine the entire beam profile and hence the total maximum power. Estimates of the total power output, based on measured profiles of an electrically excited system, indicated power levels in excess of 200 W. Estimates of the energy deposited in the laser volume (ref. 16) indicated an extraction efficiency of the order of 5 percent.

### Large-Volume Excitation of $^3\text{He}$ and Noble Gas Systems

Scaling of direct nuclear-pumped lasers using the  $^3\text{He}(n,p)^3\text{H}$  reaction could have been accomplished in a number of ways, such as increasing the thermal neutron flux, increasing the gas pressure in the laser, and increasing the volume of the laser. It did not appear reasonable to attempt to increase the thermal flux beyond that achievable with present-day fast-burst reactors. It would have been preferable, in fact, to find laser systems which would operate in a continuous mode, since they would require a much lower flux level comparable to that available in steady-state reactors. Scaling to higher pressures was limited because of collisional broadening of the upper laser level as well as collisional deactivation of this level. Therefore, to demonstrate high-power lasing with a direct nuclear-pumped laser, the Langley research group decided to increase the volume of the excited media (ref. 42). A primary concern in making this decision was the effects of plasma instability in a large-volume system, since no information on this phenomenon was available at that time.

Figure 22 is a diagram of the large-volume multiple-pass box laser assembly. A stainless steel frame with internal dimensions of  $0.40 \times 0.30 \times 0.03 \text{ m}$  was constructed. Aluminum cover plates were bolted to both sides and were covered by 0.05-m-thick polyethylene to moderate the fast neutrons. At opposite ends of the steel frame, quartz windows at the Brewster angle were attached. Two flat gold mirrors were mounted on the internal walls of the steel frame. The optical cavity

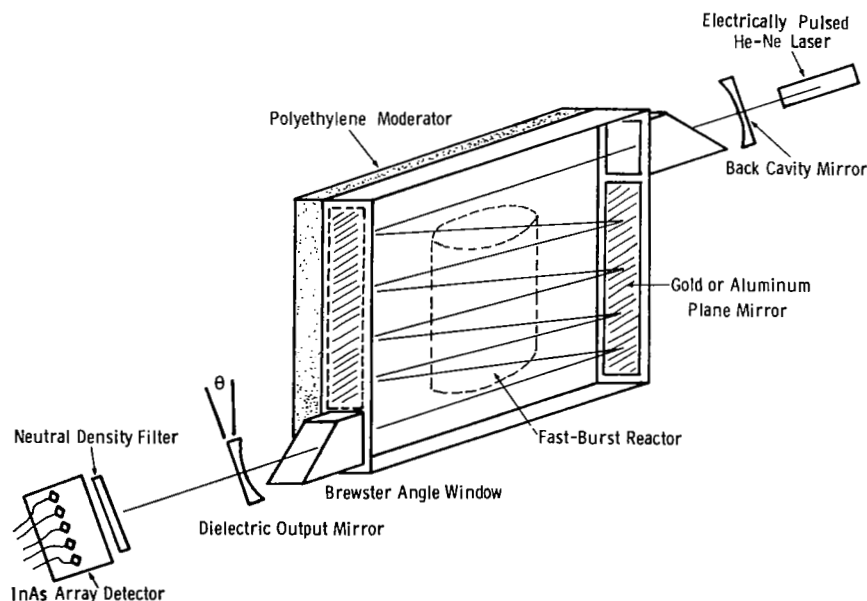


Figure 22.- Multiple-pass box laser assembly.

was formed by two 0.05-m-diameter dielectric mirrors with a 10-m radius of curvature. The back mirror was coated for maximum reflectivity and the output mirror was coated for 85-percent reflectivity at 1.79  $\mu\text{m}$ . By changing the angle  $\theta$  of these dielectric mirrors, the number of passes through the excited laser medium could be varied. A He-Ne laser (0.63  $\mu\text{m}$ ) was used to align the optical components. The system was operated with a  $^3\text{He}$ -Ar mixture (1 percent Ar) at total pressures from 80 to 290 kPa. Lasing occurred on the 1.79- $\mu\text{m}$  line of ArI and was detected by a 13-element InAs array in the form of a cross. With this detector, the intensity distribution in the laser beam could be determined. A typical result is shown in figure 23 where the output of each InAs element is shown. The signals from the individual InAs elements followed the thermal neutron flux in time. The absence of erratic behavior in the laser output indicated no gross plasma instabilities. The lasing duration of approximately 300  $\mu\text{s}$  (FWHM) indicated continuous lasing.

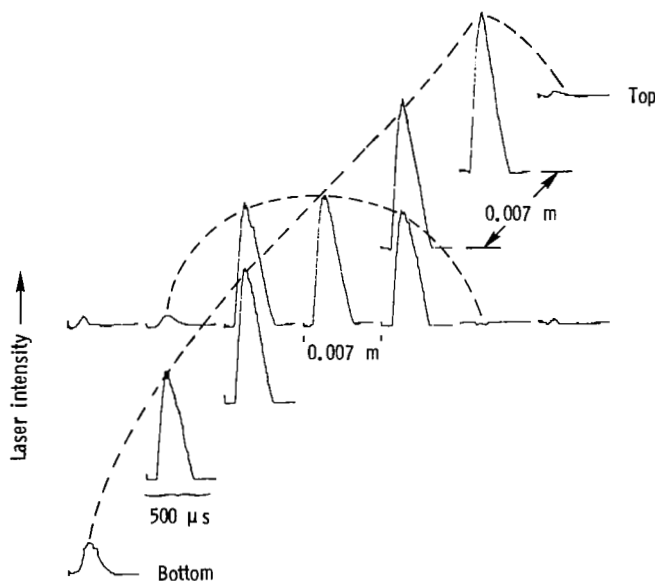


Figure 23.- Output from multiple-pass box laser ( $^3\text{He}$ -Ar).  
 Signals from the 13 detector elements shown. 1 percent  
 Ar;  $p = 200$  kPa;  $\phi = 2.7 \times 10^{20}$   $\text{n/m}^2\text{-s}$ .

In figure 24 the beam profile at a distance of 4 m from the output mirror is shown superimposed on the output Brewster angle window aperture. The beam profile fills the entire aperture; thus the laser did not operate in the fundamental mode. Higher output powers could probably have been obtained with larger apertures.

Figure 25 shows the scaling of the  $^3\text{He}$ -Ar laser output with thermal neutron flux for five passes at a total pressure of 80 kPa (2 percent Ar). The laser power scales directly with the thermal neutron flux. The circles and triangles indicate two different runs with the same experimental conditions. The data indicated a thermal neutron flux lasing threshold near  $10^{20}$   $\text{n/m}^2\text{-s}$ . This threshold, lower than that observed for the same system in a cylindrical geometry, indicated improved coupling between the reactor neutron source and the gaseous media.

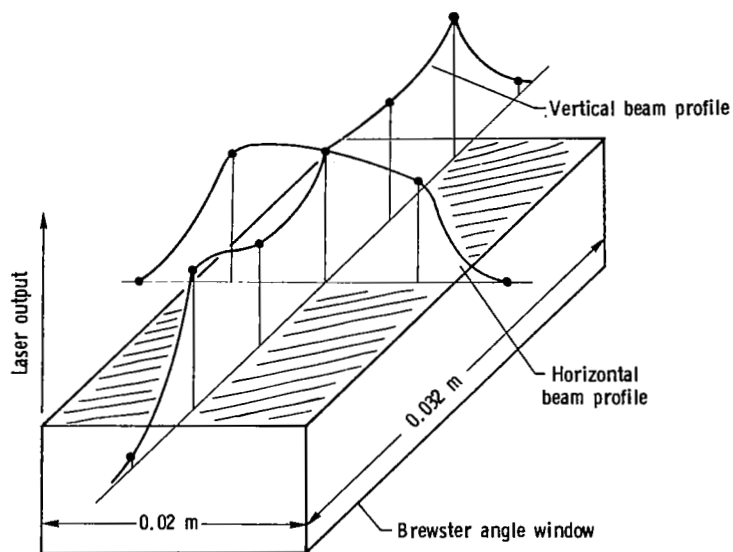


Figure 24.- Beam profile of multiple-pass box laser ( $^3\text{He-Ar}$ ). 1 percent Ar;  $p = 300$  kPa; 5 passes;  $\phi = 2.7 \times 10^{20}$   $\text{n/m}^2\text{-s}$ .

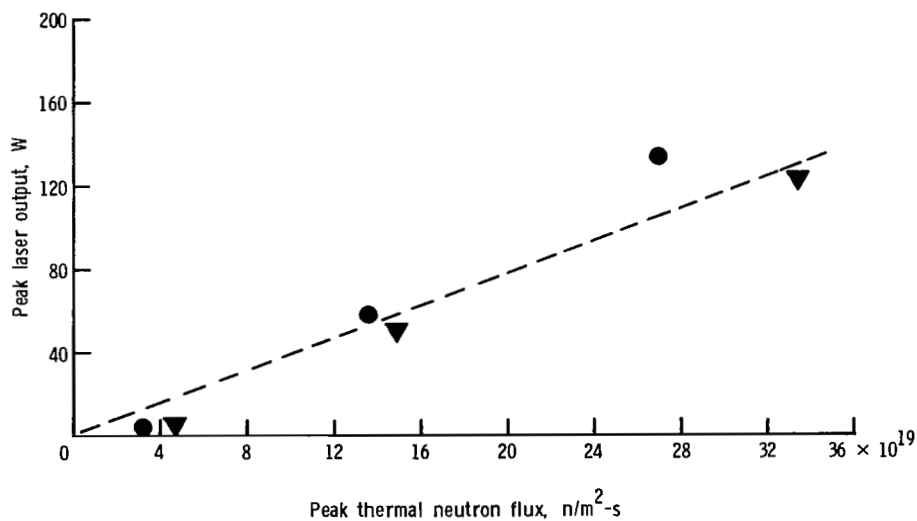


Figure 25.-  $^3\text{He-Ar}$  box laser output versus thermal neutron flux. 2 percent Ar;  $p = 80$  kPa; 5 passes.

Figure 26 shows the scaling of this system with total pressure up to 250 kPa. The different data points represent two runs with the same experimental conditions and show linear scaling of the laser output. The conditions were a peak thermal flux of  $2.8 \times 10^{20}$   $\text{n/m}^2\text{-s}$ , five passes, and 1 percent Ar.



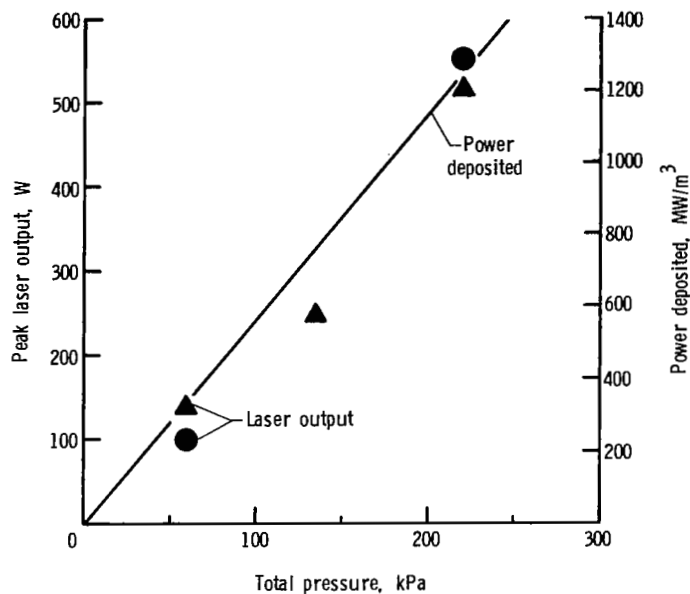


Figure 26.-  $^3\text{He-Ar}$  box laser output versus total pressure. 1 percent Ar; 5 passes;  $\phi = 2.8 \times 10^{20} \text{ n/m}^2\text{-s}$ .

Figure 27 shows the scaling of the laser output with the number of passes through the excited medium. These data indicated that five to seven passes were near optimum for peak laser output. A low number of passes did not effectively sweep out the excited volume, whereas a large number of passes resulted in high diffraction losses.

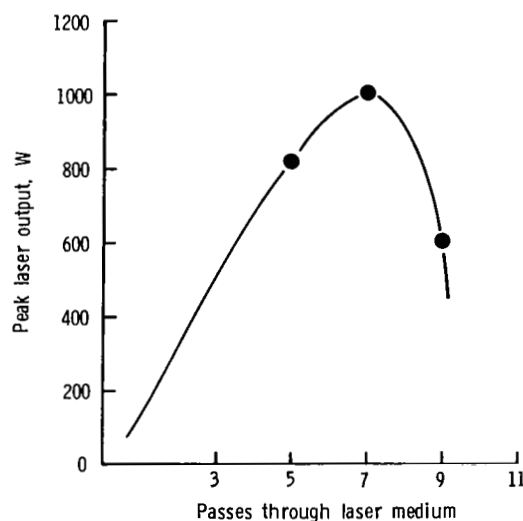


Figure 27.-  $^3\text{He-Ar}$  box laser output versus number of passes through excited medium. 0.7 percent Ar;  $p = 300 \text{ kPa}$ ;  $\phi = 4.3 \times 10^{20} \text{ n/m}^2\text{-s}$ .

Peak laser output for this system was 1012 W, obtained at a total pressure of 300 kPa (0.74 percent Ar), seven passes, and a peak thermal neutron flux of  $4.3 \times 10^{20}$  n/m<sup>2</sup>-s (ref. 43). This experiment also demonstrated the advantages of using large volumes in nuclear-pumped lasers.

#### Direct Nuclear-Pumped Oscillator and Amplifier

A standard method of increasing the power output of a laser system is amplification of the laser beam. This method was investigated to determine whether nuclear-powered amplifiers were a viable means of scaling these lasers to high powers. The arrangement of the amplifier and oscillator tubes is shown in figure 28. Both tubes were placed in a single moderator constructed of polyethylene that thermalized the neutrons produced by the fast-burst reactor. The moderator was 0.30 m high by 0.15 m wide and 0.60 m long. The tubes were located in 0.05-m by 0.05-m holes through the moderator. The lower tube, used as an oscillator, was constructed of 0.025-m i.d. stainless steel tubing. The upper tube, used as an amplifier, was constructed of 0.032-m i.d. stainless steel tubing. The ends of both tubes were cut at the Brewster angle and sealed with calcium fluoride (CaF<sub>2</sub>) windows. Both tubes had an overall length of 0.90 m. The oscillator cavity consisted of a 0.05-m-diameter flat mirror which was dielectric coated for a reflectance of 99.9 percent at 2.63  $\mu$ m. The output mirror, 0.05 m in diameter with a 10-m radius of curvature, was dielectric coated for a reflectance of 95.0 percent at 2.63  $\mu$ m. The two front surface mirrors were used to deflect the output beam of the oscillator through 180° and along the centerline of the amplifier tube. The system was aligned with a small He-Ne CW laser. Initial experiments were carried out on a <sup>3</sup>He-Xe (5 percent Xe) mixture at 80 kPa. Lasing occurred on the 2.63- $\mu$ m XeI transition, which had been previously studied. The gain of the oscillator was measured, as previously described, by inserting neutral density filters into the cavity until lasing stopped. All other parameters (Xe concentration, total pressure, and thermal neutron flux) were held constant. The gain was measured to be 125 percent/m at a total pressure of 80 kPa and a peak thermal neutron flux of  $6 \times 10^{20}$  n/m<sup>2</sup>-s.

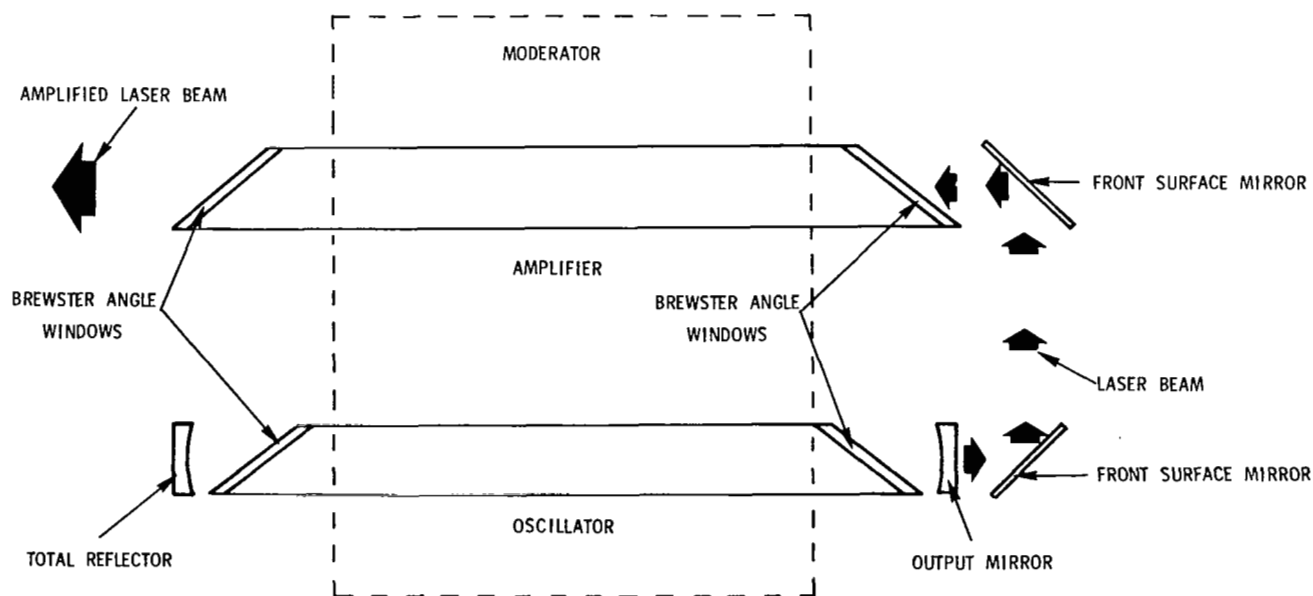


Figure 28.- Direct nuclear-pumped oscillator and amplifier.

Figure 29 compares the measured beam profiles of the oscillator output beam and the amplifier output beam. The oscillator output beam profile was obtained with the beam passing through the amplifier, but with no gas in the amplifier tube. The amplifier tube was then filled to a total pressure of 80 kPa with 5 percent Xe and 95 percent  $^3\text{He}$  (identical to the pressure and mixture in the oscillator tube). The reactor was pulsed at the same yield (thermal flux of  $6 \times 10^{20} \text{ n/m}^2\text{-s}$ ) and a second profile was obtained. The power output of the oscillator plus amplifier is a factor of 3 greater than the power output of the oscillator alone.

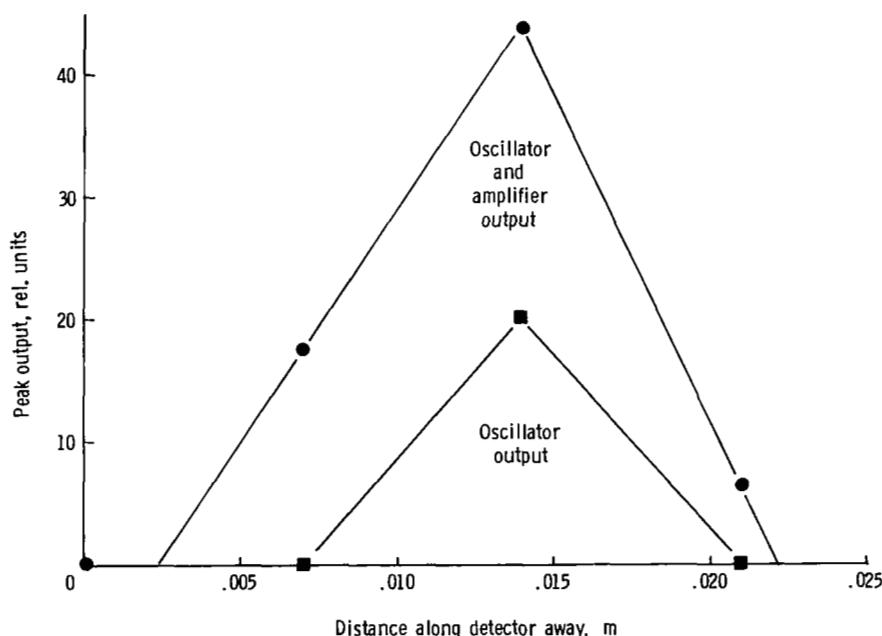


Figure 29.- Beam profiles of oscillator alone and of oscillator and amplifier.

The system was also operated with a mixture of  $^3\text{He-CO}$  (5 percent CO), which lased at approximately  $5 \mu\text{m}$ . A power amplification of a factor of 5 was obtained for this system (ref. 44). These results verified that nuclear-pumped amplifiers are a useful approach to the development of high-power nuclear-pumped lasers.

#### Other Systems Investigated

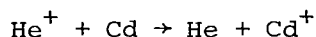
Several other systems were investigated, although lasing was achieved in only one. Initial reactor experiments were carried out with a  $^3\text{He-Ne-O}_2$  mixture which lases (electrically) at  $0.8446 \mu\text{m}$  (OI). Gain had been measured in this system when it was exposed to a thermal neutron flux of  $2.5 \times 10^{19} \text{ n/m}^2\text{-s}$  (ref. 31), but no evidence of lasing was detected in the reactor experiments.

A second system, investigated extensively by several different groups, was the  $^3\text{He-CO}_2$  laser. The high power output and high efficiency of this system when electrically pumped made it a most attractive candidate for nuclear-pumped experiments.

The first experiments on nuclear pumping of  $^3\text{He-CO}_2$  were done with a hybrid system employing both electrical and nuclear excitation. Allario et al. (ref. 23) observed an enhancement of the laser output when it was placed in a thermal neutron flux of approximately  $10^{12} \text{ n/m}^2\text{-s}$ . Andriakhin et al. (ref. 24) used a proton beam as an ionization source for a  $^3\text{He-N}_2\text{-CO}_2$  laser system and observed a considerable increase in laser power output. Excitation by the proton beam alone did not produce lasing. Using a pulsed reactor, Batyrbekov et al. (refs. 45 and 46) carried out experiments with a  $^3\text{He-N}_2\text{-CO}_2$  laser at atmospheric pressure. They observed lasing when the system, with a non-self-sustaining electrical discharge, was exposed to a neutron flux of  $5 \times 10^{20} \text{ n/m}^2\text{-s}$ . McArthur et al. (ref. 47) measured a small signal gain of 4.0 percent/m in an atmospheric pressure  $^3\text{He-N}_2\text{-CO}_2$  amplifier with a fast neutron flux of approximately  $4 \times 10^{22} \text{ n/m}^2\text{-s}$ . Gain was observed only when an electrical sustainer field was applied.

Experiments were carried out over a period of 2 years in an attempt to produce a  $^3\text{He-CO}_2$  laser excited only by nuclear reaction. No experimental evidence to indicate lasing was found. In experiments (ref. 48) using a CW  $\text{CO}_2$  laser as a probe to study the nuclear-induced plasma, Jalufka concluded that the lower laser level was probably populated by electron impact in these devices. This result indicated that direct nuclear pumping of a  $\text{CO}_2$  laser was not feasible.

Experiments on a  $^3\text{He-Cd}$  system were carried out to study the feasibility of charge exchange lasers as candidates for direct nuclear pumping. This laser operated on the charge exchange reaction:



The electrically pumped system lased on two lines, at  $0.5337 \mu\text{m}$  and  $0.5378 \mu\text{m}$ . The partial pressure of Cd was produced by heating the laser tube (with metallic Cd inside) to temperatures up to  $1100 \text{ K}$ . Total pressures of  $80 \text{ kPa}$  and thermal neutron fluxes of up to  $1.5 \times 10^{21} \text{ n/m}^2\text{-s}$  were used. Strong emission at the two laser wavelengths was observed in the reactor experiments, but no conclusive evidence of lasing was obtained. Recently Mis'kevich et al. (ref. 49) in the Soviet Union reported successful lasing of the  $^3\text{He-Cd}$  nuclear-pumped laser with much the same conditions described above except that lasing occurred at a much lower thermal neutron flux ( $\approx 10^{18} \text{ n/m}^2\text{-s}$ ). Output power obtained was about  $0.1 \text{ W}$  at  $53 \text{ kPa}$ .

Reactor experiments to investigate lasing in FI at  $0.7039 \mu\text{m}$  and  $0.7129 \mu\text{m}$  using a mixture of  $^3\text{He-NF}_3$  were also carried out. Experiments over a range of pressures (up to  $80 \text{ kPa}$ ), concentrations (up to 10 percent  $\text{NF}_3$ ), and thermal neutron flux (up to  $1.5 \times 10^{21} \text{ n/m}^2\text{-s}$ ) produced no evidence of lasing.

Experiments using a mixture of 1 percent Xe, 1 percent  $\text{NF}_3$ , and 98 percent  $^3\text{He}$  at a total pressure of  $200 \text{ kPa}$  were carried out with a mirror set dielectric coated for  $0.3550 \mu\text{m}$ . This was an attempt to study a nuclear-pumped  $\text{XeF}$  excimer laser. No lasing was observed, although strong fluorescence was observed.

### Summary of $^3\text{He}$ Experiments

The use of  $^3\text{He}$  as a volumetric excitation source resulted in the successful demonstration of several nuclear-pumped lasers. These successes led to a better understanding of the many atomic and molecular processes occurring in a radiation-induced plasma and also demonstrated that a high-power laser excited only by nuclear

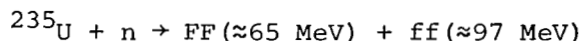
reactions was achievable. Most of the lasers that were demonstrated were recombination lasers, which have a low quantum efficiency and are not the best candidates for a high-power, high-efficiency space-based laser system. Much more research is required in this area to determine the best candidate for scaling to higher powers. This will require extensive studies of the many atomic and molecular processes in the plasma in order to decide which population inversion mechanisms will produce more efficient lasers. Until these questions are resolved, scaling of these systems to higher powers does not appear to be reasonable.

#### DIRECT NUCLEAR-PUMPED LASERS USING FISSIONABLE WALL COATINGS

Another class of direct nuclear-pumped lasers which were successfully demonstrated relied on a coating of fissionable material such as uranium or boron on the inside of the laser tube. When these systems were exposed to a thermal neutron flux, the reaction



or



takes place. In these reactions,  $n$  is a thermal neutron,  $\alpha$  is an alpha particle, FF is a heavy fission fragment, and ff is a light fission fragment. The coated-tube technique was based on surface emission of energetic particles; thus, high-pressure operation was limited because the stopping distance of the energetic particles became too small in relation to the laser tube diameter. This technique did have the advantage of allowing gases to be tested without the addition of He, and because of the higher energy of the fission fragments, adequate energy deposition could be obtained at lower neutron fluxes and gas pressures. The major disadvantages of using wall coatings were that

1. Less than half of the fission energy was absorbed in the gas.
2. Energy deposition was nonhomogeneous.
3. Uniform coatings were difficult to produce.
4. Scaling to high pressures was not feasible.

#### CO System

The first successful demonstration of a direct nuclear-pumped laser was achieved by McArthur and Tollefsrud (ref. 27). In these experiments, pure CO at 77 K was excited by fission fragments produced by a  $^{235}\text{U}_3\text{O}_8$  coating that had been exposed to the moderated neutron flux produced by a fast-burst reactor. Lasing occurred in the 5.1- $\mu\text{m}$  to 5.6- $\mu\text{m}$  vibrational bands of CO. Total CO pressures of 13.3 kPa were used in these experiments and a total power output of 2 to 6 W was achieved.

Later experiments by McArthur (ref. 50), using a "folded-path" laser to extend the gain length, produced a peak power of approximately 100 W. McArthur also experimented with CO-Ar mixtures and observed a lower lasing threshold ( $5 \times 10^{20}$ ) for a

50 percent CO, 50 percent Ar mixture. Lasing at room temperature (300 K) was also observed with the CO-Ar mixture, but the power output was low.

#### <sup>4</sup>He and Noble Gas Systems

Helmick, Fuller, and Schneider (ref. 28), using a <sup>235</sup>U metal lining in the laser tube, observed lasing on the XeI transition at 3.508  $\mu\text{m}$  ( $5d[7/2]_3^0 - 6p[5/2]_2$ ). These experiments used a 0.30-m-long quartz laser tube (0.019-m i.d.) and a cavity formed by a flat silver alloy reflector and a 4-m radius of curvature silver alloy reflector. The reflectors were placed 1.18 m apart, and output coupling was through a 0.001-m-diameter hole in the spherical reflector. The Godiva IV fast-burst reactor at Los Alamos Scientific Laboratories was used to produce a pulsed fast-neutron flux ( $\approx 150 \mu\text{s}$  FWHM). Gas mixtures of <sup>4</sup>He-Xe in a ratio of 200:1 at a total pressure of 27 kPa were initially employed, but concentration studies showed improved output at a 20:1 mixing ratio. The behavior of the laser output exhibited a sharp threshold at  $5 \times 10^{17} \text{ n/m}^2\text{-s}$  with the laser output following the thermal neutron flux. A peak power of at least 10 mW was obtained in these experiments.

Voinov et al. (ref. 35) observed lasing on the XeI ( $5d[5/2]_2^0 - 6p[5/2]_2$ ) transition at 2.627  $\mu\text{m}$  using a cell constructed of two  $2.0 \times 0.06 \text{ m}$  flat aluminum plates. These plates were 0.02 m apart and their inside surfaces were coated with a layer of <sup>235</sup>U urano-uranic oxide to a thickness of 30 mg/m<sup>2</sup>. The average thermal neutron flux over the cell length was  $1.1 \times 10^{19} \text{ n/m}^2\text{-s}$ . The neutron pulse length was about 4 ms (FWHM). The laser cavity was formed by a 10-m radius of curvature and a flat ( $R = 0.77$ ) dielectric-coated mirror of 0.03-m diameter. A gas mixture of <sup>4</sup>He-Xe (1000:1) and total pressures up to 400 kPa were used. A peak power of 250 W was obtained at 300 kPa. Extraction efficiency ranged from 0.9 to 1.2 percent. A minimum thermal neutron flux lasing threshold of  $6.0 \times 10^{17} \text{ n/m}^2\text{-s}$  was determined for a resonator consisting of two flat ( $R = 0.99$ ) mirrors and a total pressure of 100 kPa.

Investigation (ref. 35) of an Ar-Xe gas mixture (500:1) at a total pressure of 50 kPa produced lasing at 2.627  $\mu\text{m}$  ( $5d[5/2]_2^0 - 6p[5/2]_2$ ), 2.482  $\mu\text{m}$  ( $5d[5/2]_3^0 - 6p[5/2]_3$ ), and 2.026  $\mu\text{m}$  ( $5d[3/2]_1 - 6p[3/2]_1$ ). Total peak power achieved in these experiments was 130 W at an extraction efficiency of approximately 1 percent. The laser pulse duration was 12.5 ms and the thermal neutron flux lasing threshold was  $8.0 \times 10^{16} \text{ n/m}^2\text{-s}$ . Lasing in XeI at 3.108  $\mu\text{m}$  ( $5d[5/2]_3^0 - 6p[3/2]_2$ ) was also observed in these experiments with different cavity mirrors. The change in spectral and threshold characteristics when the helium was replaced with argon was probably due to a change in the mechanism producing the upper laser level. In He-Xe mixtures, the upper laser level was produced by collisional-radiative recombination, whereas in the Ar-Xe mixtures, the upper laser level was produced by collisional energy transfer from metastable argon atoms and molecules with xenon atoms.

Voinov et al. (ref. 36) also carried out nuclear-pumped experiments on Ar, Kr, and Xe mixtures using a cylindrical laser cell of 0.027 m i.d. and 0.57 m long. The inner surface of the cell was coated with <sup>235</sup>U urano-uranic oxide to a thickness of about 90 g/m<sup>2</sup>. A peak thermal neutron flux of  $5.25 \times 10^{20} \text{ n/m}^2\text{-s}$  with a FWHM of 0.8 ms was used.

Gas mixtures consisting of <sup>4</sup>He-Ne, <sup>4</sup>He-Ar, Ne-Ar, <sup>4</sup>He-Kr, Ne-Kr, Ar-Kr, <sup>4</sup>He-Xe, Ne-Xe, Ar-Xe, and Kr-Xe were studied at a total pressure of 100 kPa and mixtures

varying from 200:1 to 200:30. Lasing was achieved in  $^4\text{He-Ar}$  at  $2.397\text{ }\mu\text{m}$  ( $3d[1/2]_0^0 - 4p[1/2]_1$ ),  $1.19\text{ }\mu\text{m}$  ( $3d[5/2]_2^0 - 4p[3/2]_2$ ), and  $1.149\text{ }\mu\text{m}$  ( $4p[1/2]_1 - 4s[1/2]_1^0$ ), in  $^4\text{He-Kr}$  at  $2.523\text{ }\mu\text{m}$  ( $4d[1/2]_1^0 - 5p[3/2]$ ), and in  $^4\text{He-Xe}$  at  $2.627\text{ }\mu\text{m}$  ( $5d[5/2]_2^0 - 6p[5/2]_2$ ) and  $2.483\text{ }\mu\text{m}$  ( $5d[5/2]_2^0 - 6p[5/2]_2$ ). Lasing in mixtures of Ar-Kr, Ar-Xe, and Kr-Xe was also achieved in the range from 2 to  $10\text{ }\mu\text{m}$ , but the output spectra for these mixtures were not studied in detail.

The output energy as a function of total pressure was investigated (ref. 36) for the  $^4\text{He-Ar}$  and the  $^4\text{He-Xe}$  lasers. Total pressures ranged up to 400 kPa for  $^4\text{He-Ar}$  and 500 kPa for  $^4\text{He-Xe}$ . The  $^4\text{He-Xe}$  system produced considerably more power (2 kW at  $2.63\text{ }\mu\text{m}$ ) than the  $^4\text{He-Ar}$  system at all pressures, and peak output occurred for the  $^4\text{He-Ar}$  system at approximately 200 kPa and for the  $^4\text{He-Xe}$  system at approximately 400 to 500 kPa. The cavity for the  $^4\text{He-Ar}$  system consisted of a total reflector with a 10-m radius of curvature and a flat output reflector of  $R = 0.94$ , whereas the  $^4\text{He-Xe}$  cavity consisted of a total reflector with a 10-m radius of curvature and a flat output reflector with  $R = 0.77$ . The behavior of these systems was the same as that observed earlier with  $^4\text{He-Xe}$ . The laser output followed the thermal neutron pulse and displayed a sharp lasing threshold, at  $10^{20}\text{ n/m}^2\text{-s}$  for the  $^4\text{He-Ar}$  laser and at  $10^{19}\text{ n/m}^2\text{-s}$  for the  $^4\text{He-Xe}$  laser.

#### Ne-N<sub>2</sub> System

Direct nuclear pumping of a Ne-N<sub>2</sub> system has been observed by De Young et al. (ref. 29). Lasing occurred simultaneously at  $0.8629\text{ }\mu\text{m}$  ( $\text{NI}, 3p^2P_{3/2}^0 - 3s^2P_{3/2}$ ) and  $0.9392\text{ }\mu\text{m}$  ( $\text{NI}, 3p^2D_{5/2}^0 - 3s^2P_{3/2}$ ). The laser cell consisted of a quartz tube containing a 0.68-m-long aluminum cylinder (0.025-m i.d.) coated on the inner surface with  $^{10}\text{B}$ . The ends of the quartz tube were cut at the Brewster angle. The laser cavity was formed by a 2-m radius of curvature mirror dielectric coated for a reflectance of 0.999 and a 1-m radius of curvature output mirror dielectric coated for a reflectance of 0.995 at  $0.8446\text{ }\mu\text{m}$ . The mirror separation was 0.87 m. The cavity also contained a chopping fan in front of the back mirror. This fan was driven by an electric motor so that the mirror was alternately blocked and unblocked during the reactor pulse. Neutrons were produced in a pulse mode by a TRIGA reactor. A peak flux of approximately  $10^{20}\text{ n/m}^2\text{-s}$  with a FWHM of 12 ms was obtained. The thermal flux lasing threshold was approximately  $10^{19}\text{ n/m}^2\text{-s}$ .

Total pressure ranged from 10 to 50 kPa in these experiments with a partial pressure of N<sub>2</sub> of only a 0.10 Pa. A total laser output of 1.5 mW was obtained for an extraction efficiency of approximately  $1.4 \times 10^{-4}$  percent (at 20 kPa).

Experiments were also carried out on this system using  $^{235}\text{U}$ -coated cylinders in place of the  $^{10}\text{B}$ -coated cylinders. Lasing was achieved over a pressure range from 13.3 to 37.0 kPa with a N<sub>2</sub> partial pressure less than 1.33 Pa. Laser output was lower for this system than for the  $^{10}\text{B}$ -coated system.

The excitation mechanism for this laser was collisional-radiative recombination (ref. 51).

### He-Hg System

Lasing on the  $0.6150 \mu\text{m}$  ( $\text{HgII}, 7p^2P_{3/2} - 7s^2S_{1/2}$ ) transition was observed in an He-Hg mixture by Akerman et al. (ref. 52). The laser cell was constructed of a  $0.027\text{-m}$  i.d. pyrex tube  $0.86\text{ m}$  long. The tube ends were cut at the Brewster angle and sealed with quartz windows. The cell contained  $0.60\text{ m}$  of  $0.0254\text{-m}$  o.d. titanium tubing coated on the inside with a  $4.0\text{ g/m}^2$  layer of  $66.8$  percent (by weight)  $^{10}\text{B}$ . The tube was wrapped with heating tape so that the partial pressure of mercury in the cell could be controlled. The laser cavity consisted of a  $3\text{-m}$  radius of curvature back mirror dielectric coated for a reflectance of  $0.999$  and a flat output mirror dielectric coated for a reflectance of  $0.990$ .

Total gas pressure ranged from  $40$  to  $80\text{ kPa}$ . Partial pressure of mercury ranged from  $0.27$  to  $1.0\text{ Pa}$ . Peak thermal neutron fluxes were varied from  $2.5 \times 10^{20}$  to  $4.8 \times 10^{20}\text{ n/m}^2\text{-s}$ . The thermal flux lasing threshold was  $10^{20}\text{ n/m}^2\text{-s}$ . The peak laser output of approximately  $1\text{ mW}$  obtained at  $80\text{ kPa}$  in these measurements gave an extraction efficiency of approximately  $10^{-6}$  percent. Of all the nuclear-pumped lasers demonstrated, this one had the shortest wavelength. The mechanism by which the upper laser level was populated was not definitely known, but was thought to be charge exchange of Hg with the  $\text{He}^+$  ion.

Earlier reports of lasing in mercury have been reported by Andriakhin et al. (ref. 53). However, experiments carried out by Akerman et al. under the conditions reported by Andriakhin did not produce lasing.

### $^4\text{He-CO}$ and $^4\text{He-CO}_2$ Systems

Prelas et al. (ref. 54) observed lasing at  $1.45 \mu\text{m}$  ( $\text{CI}, 3p^1P_1 - 3s^1P_1$ ) in He-CO and He-CO<sub>2</sub> mixtures using the  $^{10}\text{B}(n,\alpha)^7\text{Li}$  reaction. The experimental arrangement was essentially the same as that used by Akerman et al. (ref. 52). The cavity was formed by two  $3\text{-m}$  radius of curvature mirrors dielectric coated for a reflectivity of  $0.999$  at  $1.45 \mu\text{m}$ . The mirrors were separated by a distance of  $1.17\text{ m}$ . Lasing occurred at total pressures of  $6.7$ ,  $27$ , and  $80\text{ kPa}$  with the partial pressure of CO being about  $0.1\text{ Pa}$  and that of CO<sub>2</sub> being  $0.3\text{ Pa}$ .

An interesting phenomenon was observed in these experiments at a total pressure between  $6.7$  and  $27\text{ kPa}$ . The peak laser output signal occurred up to  $5\text{ ms}$  (at  $10\text{ kPa}$ ) after the peak neutron flux. The delay was observed to be pressure dependent and is thought to be due to multiple collision processes which populate the upper laser level. These experiments were carried out using a TRIGA reactor at a thermal neutron flux of  $2.5 \times 10^{19}\text{ n/m}^2\text{-s}$ . The FWHM of the neutron pulse was  $12\text{ ms}$  and lasing continued for up to  $20\text{ ms}$ . A thermal neutron threshold flux of approximately  $4 \times 10^{18}\text{ n/m}^2\text{-s}$  was measured, but no measurement of power output was reported.

### Ar-Xe Multiple-Pass System

Nuclear-pumped lasing of an Ar-Xe (9:1) mixture in a multiple-pass laser using  $^{235}\text{U}_3\text{O}_8$  coatings was reported by De Young (ref. 55). Lasing occurred at  $2.6 \mu\text{m}$  ( $\text{XeI}, 5d[3/2]_1^0 - 6p[1/2]_0$  and  $5d[5/2]_2^0 - 6p[5/2]_2$ ), at a total pressure of  $100\text{ kPa}$  and a thermal neutron flux of  $3.5 \times 10^{20}\text{ n/m}^2\text{-s}$ .





L-80-4230

Figure 30.- Multiple-pass wall-coated laser assembly.

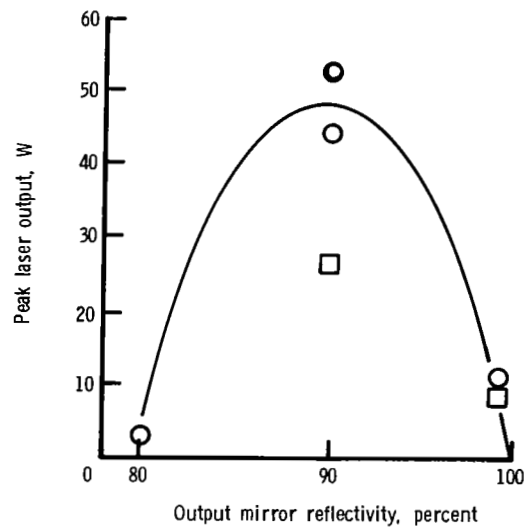


Figure 31.- Multiple-pass Ar-Xe laser output versus output mirror reflectivity. 10 percent Xe;  
 $p = 93 \text{ kPa}$ ;  $\phi = 3.5 \times 10^{20} \text{ n/m}^2\text{-s}$ .

The laser system is shown in figure 30. The inside of 0.025-m i.d. ceramic tubes were coated with  $^{235}\text{U}_3\text{O}_8$ . The total path length through the excited medium was 2.4 m. Figure 31 shows the variation of laser output as a function of output mirror reflectivity. The back mirror had a reflectivity of 0.995. The test-point symbols indicate different runs under similar experimental conditions. The variation of laser output with xenon concentration is shown in figure 32. Optimum concentration for this system was about 10 percent Xe, which was considerably different from the  $^3\text{He-Xe}$  system. The variation of laser output with total pressure is shown in figure 33. As the total pressure increased, the range of the fission fragments decreases, so that at pressures above 100 kPa (when the range of the fission

fragments was about equal to the tube diameter), the laser output decreased rapidly. A peak power output of 50 W was measured at optimum conditions.

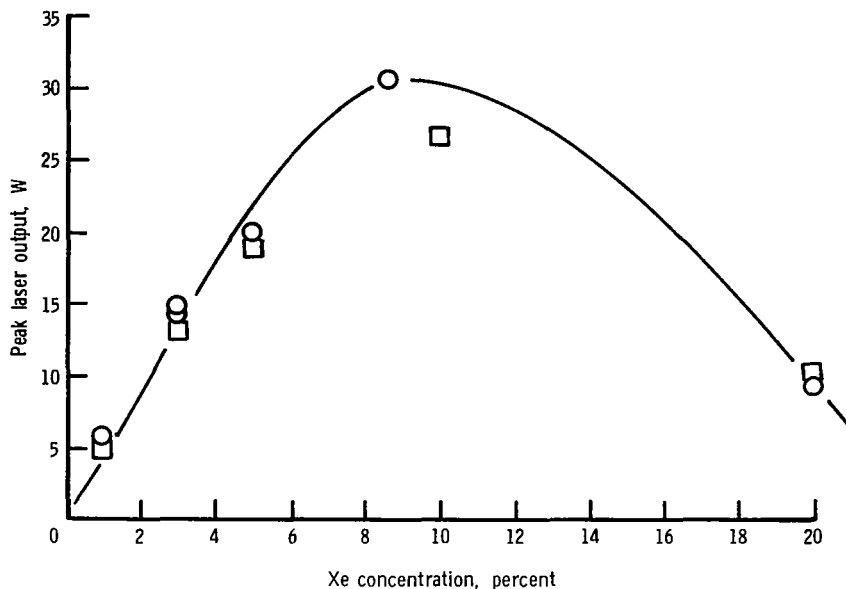


Figure 32.- Multiple-pass Ar-Xe laser output versus Xe concentration. Output mirror reflectivity, 99 percent;  $p = 80$  kPa;  $\phi = 5 \times 10^{20}$  n/m<sup>2</sup>-s.

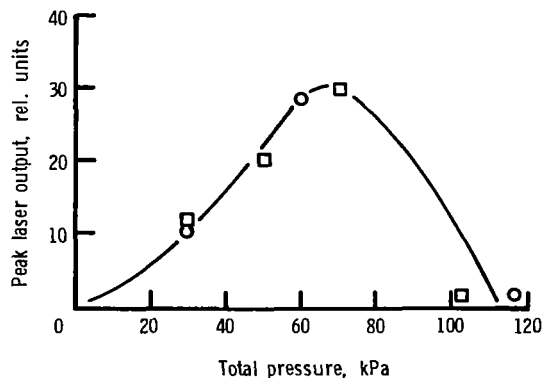


Figure 33.- Multiple-pass Ar-Xe laser output versus total pressure. Output mirror reflectivity, 90 percent; 10 percent Xe;  $\phi = 5 \times 10^{20}$  n/m<sup>2</sup>-s.

#### Other Experiments

Miley (ref. 56) carried out an investigation which produced some interesting results, but in which lasing was not achieved. This investigation measured the gain in a XeF excimer system excited by the  $^{10}\text{B}(n,\alpha)^7\text{Li}$  reaction. Mixtures of Ar-Xe-NF<sub>3</sub> in the ratio 99.34 percent:0.5 percent:0.16 percent at a total pressure of 40 kPa were exposed to a thermal neutron flux produced by moderation of the fast flux from a TRIGA reactor. Although the energy deposition in these experiments was only about

40 MW/m<sup>3</sup> (below that required to achieve lasing), a stimulated to spontaneous emission ratio of about 8 was observed, indicating efficient formation of the XeF excimer. This system was of particular interest since it is one of a few systems studied that required fluorine and may therefore be compatible with <sup>235</sup>UF<sub>6</sub>, which is considered to be the most likely fuel for a self-powered reactor-laser.

### N<sub>2</sub>-CO<sub>2</sub> TRANSFER LASER

Using a transfer laser system consisting of a nuclear exciter section which excited nitrogen and a mixing section which contained <sup>4</sup>He and CO<sub>2</sub>, Rowe et al. (ref. 57) demonstrated nuclear lasing in an N<sub>2</sub>-CO<sub>2</sub> laser. In this system, the excited nitrogen was expanded through a nozzle and mixed into the CO<sub>2</sub>-He gas stream. The exciter section was coated internally with boron, and neutrons were provided by a fast-burst reactor. The system is shown in figure 34.

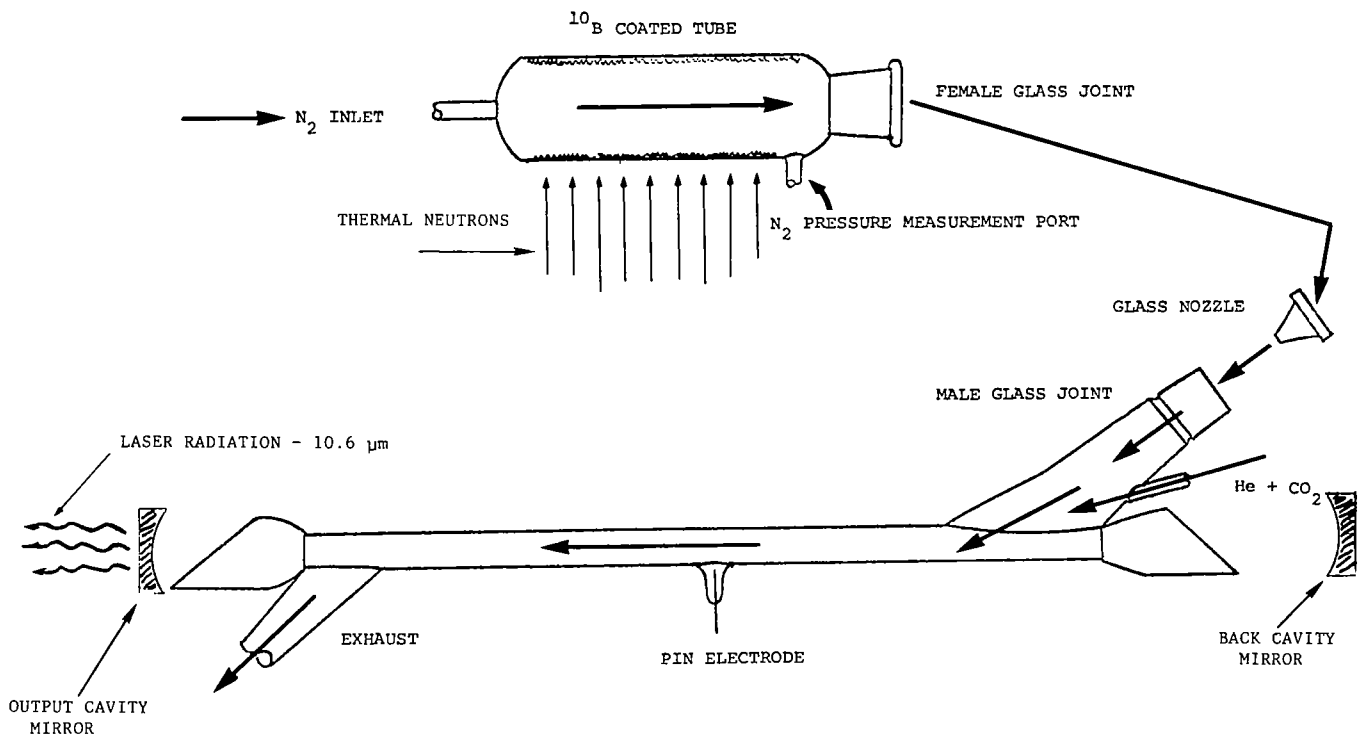


Figure 34.- N<sub>2</sub>-CO<sub>2</sub> nuclear-excited transfer laser.

The laser cavity was 0.80 m long and consisted of a flat and a 10-m radius of curvature gold-coated mirror. Output coupling was through a hole in one of the mirrors. The laser tube was 0.50 m long and 0.013 m i.d. The tube ends were sealed with NaCl Brewster angle windows. Mass flow rate in the laser was typically  $7.6 \times 10^{-4}$  m<sup>3</sup>/s. Peak thermal neutron flux of  $5 \times 10^{20}$  n/m<sup>2</sup>-s and a FWHM of 200 μs were used with pressures of 1.0 and 0.5 kPa with a mixing ratio of 1:3:8 (CO<sub>2</sub>:N<sub>2</sub>:He). The laser output pulse appeared 30 ms later than the reactor pulse. This time delay, required for the excited nitrogen to move from the exciter section to the laser tube, was consistent with the measured gas flow velocities. The laser pulse lasted 1 ms (FWHM) at 0.5 kPa and 3 ms (FWHM) at 1.0 kPa. Output power was estimated to be 100 W.

Since the  $\text{CO}_2$  was not directly exposed to the thermal flux or the resulting fission fragments, the problems associated with direct excitation of  $\text{CO}_2$  (i.e., filling of the lower laser level) were avoided. This was the only transfer laser system investigated in the nuclear-pumped laser program and was the only experiment to demonstrate lasing in  $\text{CO}_2$  using nuclear excitation.

#### DIRECT NUCLEAR-PUMPED LASERS USING $^{235}\text{UF}_6$

An important goal for nuclear-pumped laser research was the demonstration of lasing with excitation provided by the  $^{235}\text{UF}_6(n, \text{ff})\text{FF}$  reaction. At sufficient densities of gaseous  $^{235}\text{UF}_6$ , a critical system could be achieved and the need for an external neutron source eliminated. This would allow direct conversion of nuclear energy into laser emission without the conventional thermal cycle. Such a compact system would have many applications in space.

The experimental setup (ref. 58) consisted of a 0.025-m i.d. quartz tube 0.80 m long. Quartz windows at the Brewster angle were attached to the ends of the tube. The cavity was formed by dielectric mirrors having a 10-m radius of curvature and spaced 1 m apart. The back mirror had a reflectivity greater than 0.99, while the output mirror had a transmission of 0.01 at  $2.63 \mu\text{m}$ . A linear array of InAs detectors was used to resolve the laser beam profile. The neutrons were produced by a fast-burst reactor which delivered peak thermal flux pulses of  $8 \times 10^{20} \text{ n/m}^2\text{-s}$  with a FWHM of  $200 \mu\text{s}$ .

Figure 35 shows a typical output of the nuclear laser at a total pressure of 80 kPa in a mixture of Ar-Xe (0.97:0.03). Lasing occurred in XeI at  $2.65 \mu\text{m}$  ( $5d[3/2]_1^0 - 6p[1/2]_0$ ) and  $2.62 \mu\text{m}$  ( $5d[5/2]_2^0 - 6p[5/2]_2$ ) and lasted for  $300 \mu\text{s}$ , indicating steady-state operation. The size of the laser beam profile (i.e., intensity distribution), which was substantially larger than the detector array (0.015 m), suggested that lasing did not occur in just the fundamental mode, since the beam diameter for the given cavity dimensions should have been only 0.0124 m. Peak power of 4.6 W was measured at 80 kPa, and the minimum thermal flux lasing threshold was  $4 \times 10^{19} \text{ n/m}^2\text{-s}$ .

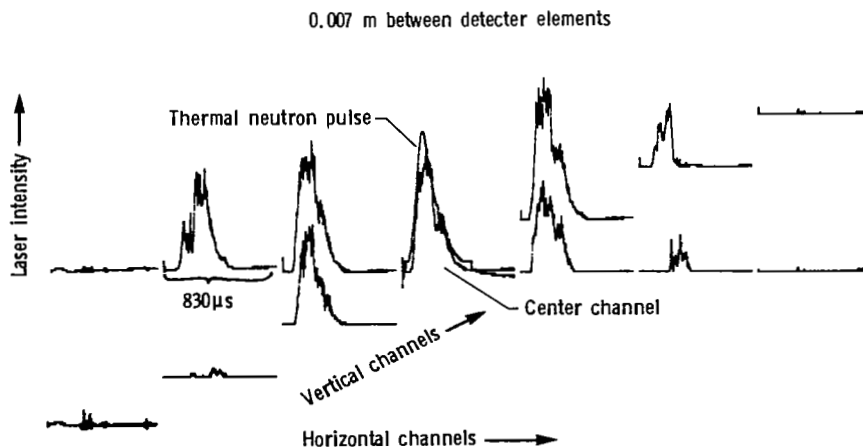


Figure 35.- Ar-Xe laser output using gaseous  $^{235}\text{UF}_6$  excitation. Signals from 13 detectors shown.

Lasing was also achieved in He-Xe mixtures, although the dominant wavelength was not determined. The He-Xe mixture did not produce as high an output as the Ar-Xe mixture at the same total pressure because the fission fragments were stopped in a much shorter distance in Xe.

Fission fragment energy deposition in the gas resulted from a combination of a uranium wall coating and gaseous  $^{235}\text{UF}_6$ . The wall coating of  $\text{UO}_2\text{F}_2$  and  $\text{UF}_4$  was formed on the inner laser cell wall by electrically pulsing gaseous  $^{235}\text{UF}_6$  at 0.67 kPa, which dissociated it into  $^{235}\text{UO}_2\text{F}_2$  and  $^{235}\text{UF}_4$ . This coating was deposited inhomogeneously on the cell wall and resulted in nonuniform excitation of the laser medium. This is apparent from the erratic lasing shown in figure 35. A fast-response pressure transducer was mounted at one end of the laser cell to measure the shock-wave pressure produced after a reactor pulse. These data allowed the mean power deposited per cubic meter to be calculated. For a mixture of Ar-Xe (3 percent Xe), a total pressure of 800 kPa, and a peak thermal flux of  $7.7 \times 10^{20} \text{ n/m}^2\text{-s}$ , the power deposited in the laser medium by the wall coating was  $18 \text{ MW/m}^3$ . With  $^{235}\text{UF}_6$  added to the mixture at a partial pressure of 0.4 kPa, the power deposited increased by 38 percent to  $25 \text{ MW/m}^2$ . The laser output, however, did not increase with additional pumping by the gaseous  $^{235}\text{UF}_6$ , probably because of quenching of  $\text{Xe}^+$  recombination by  $\text{F}^-$  ions. Formation of  $\text{F}^-$  ions depleted the free electron population and thus severely reduced the recombination rate. Collisional deexcitation of the upper laser levels by  $\text{UF}_6$  and its products may also have occurred. However, it was possible to add up to 0.4 kPa of gaseous  $^{235}\text{UF}_6$  to the laser medium without seriously quenching the laser output. The addition of 0.67 kPa of  $^{235}\text{UF}_6$  resulted in total quenching and no laser output was observed. It may be possible eventually to eliminate the wall coating and achieve lasing with only gaseous  $^{235}\text{UF}_6$  if a suitable lasing medium can be found. This experiment was the first to achieve partial pumping of the laser medium by gaseous  $^{235}\text{UF}_6$ .

#### SYSTEM STUDY

A major goal of the direct nuclear-pumped laser program was to determine whether lasers were a feasible method of extracting energy from a gas core reactor. These two research programs were basic in nature and it was only after successful demonstration of direct nuclear-pumped lasers and a gas core reactor that studies were carried out to determine the compatibility of the two systems. An excellent review article of the progress made in both gas core reactor research and nuclear-pumped laser research was published by Thom and Schneider (ref. 30).

Rodgers (ref. 59) performed an analytical study of a self-critical nuclear-pumped laser system concept. The emphasis in this study was on a reactor concept that would use  $^{235}\text{UF}_6$  as the fissioning material. The reference configuration for this study had a lasing volume of  $3.2 \text{ m}^3$  as the reactor core. Rodgers concluded from this study that a self-critical direct nuclear-pumped laser-reactor could be a very attractive candidate for a very high-power laser system if a few important technical questions could be resolved. Foremost among these questions was the identification of potential lasing systems that could function in a  $\text{UF}_6$  environment. If a suitable candidate could be found, it would be possible to produce a gas core reactor-laser system which would be self-critical and would have the potential of multimegawatt continuous power output.

Several other approaches to a laser-reactor system are discussed in the review paper by Miley (ref. 60).

## RELATED THEORY AND EXPERIMENTS

A fully time-dependent numerical model characterizing proton beam-pumped laser chemistry was developed by Fisher and Lim (ref. 61). This model was used to investigate an Ar-Kr-F<sub>2</sub> and a He-CO mixture as an aid to direct nuclear-pumped simulation experiments. These systems represented typical excimer and infrared laser systems for which substantial information existed. Major features of the model included the deposition of energy by fast protons or electrons, characterization of transient electron energy distributions, time-dependent and neutral chemistry, and multilevel energy transfer processes.

In the excimer system (Ar-Kr-F<sub>2</sub>), it was demonstrated that under low energy deposition rates, the formation of KrF\* was dominated by an excited-state mechanism, while under the high-energy deposition rates anticipated for direct nuclear-pumped operation, an ion recombination mechanism dominated the formation of KrF\*. No conclusion was made concerning the feasibility of producing a direct nuclear-pumped excimer laser.

For the infrared active He-CO system, some fundamental difficulties appeared which suggested a limitation for direct nuclear-pumped operation. Although high electron densities were produced under high energy deposition rates, the large low-energy vibrational cross sections led to rather low mean electron temperature. This condition strongly favored superelastic deactivation of the vibrational levels associated with lasing. The successful demonstration of a direct nuclear-pumped CO laser (ref. 27) was shown to be consistent with a pumping mechanism involving electronic quenching and ion recombination processes. No conditions were found in this study for which direct nuclear pumping of the CO laser system achieved the efficiency of the electrical-discharge sustainer system. This conclusion appeared to be applicable to other infrared molecular laser systems.

Davis (ref. 62) studied optical emission from Ar and Ar-N<sub>2</sub> mixtures excited by fission fragments from a <sup>235</sup>UO<sub>2</sub> coating excited by the University of Florida training reactor. This investigation was directed toward a better understanding of the methods by which fission fragment energy was deposited into a gas. The system was modeled to determine excited-state populations of the various species. Calculated values were within a factor of 10 of the experimental values, and the model adequately predicted the relative change in magnitude of the measured populations as a function of nitrogen concentration. Davis found that approximately 86 percent of the excitation produced went into the formation of nitrogen molecules in the A<sup>3</sup>Π<sub>u</sub> state. Since this was a metastable state, it served as an efficient energy storage medium.

Zapata-Casares (ref. 63) studied the collisional formation, lifetime, and quenching parameters of XeF\*(B) produced by direct fission fragment excitation. He used a <sup>252</sup>Cf source and time-resolved spectroscopy to study the emission of the XeF\* excimer (B→X transition) produced by the passage of a single fission fragment. Qualitative measurements using different gases showed Kr to be the best buffer gas at pressures below 100 kPa. A kinetic model was developed to study the processes involved in the formation and quenching of the XeF\*(B) state. Zapata concluded that for the conditions of his experiment and at pressures below 100 kPa, the XeF\*(B) state was formed predominantly by collisions between the Xe metastable atom and the fluorine donating molecule. In his experiment, NF<sub>3</sub> was used as the fluorine donor. Formation rate coefficients, inverse lifetimes, and quenching rate coefficients were determined for XeF\*, KrF\*, and Ar<sub>2</sub>\*.

De Young and Weaver (ref. 64) investigated the visible spectra emitted from a  ${}^3\text{He}(n,p){}^3\text{H}$  nuclear-induced plasma generated under high thermal neutron flux and lasing conditions. Spectra from mixtures of  ${}^3\text{He}$  and Ar, Xe, Kr, Ne,  $\text{Cl}_2$ ,  $\text{F}_2$ , and  $\text{N}_2$  were recorded with low resolution. Comparison of these spectra with those obtained from the afterglow of a high-pressure electrically pulsed plasma produced in the same gas mixtures indicated little difference in the emission. Excimer emission from  $\text{XeF}^*$  and  $\text{KrF}^*$  was also observed under  ${}^3\text{He}$  nuclear excitation, but the data were inadequate to estimate densities. Adding  ${}^{235}\text{UF}_6$  to He and Ar to excite the gas caused strong quenching of the line emission for mixtures of 10 percent  $\text{UF}_6$  and 90 percent He. These experiments pointed out the usefulness of high-pressure discharge experiments in the laboratory as a way of investigating candidate systems for nuclear-pumped lasing.

Zediker et al. (ref. 65) studied the production of  $\text{O}_2(^1\Delta)$  by nuclear pumping to determine whether it was possible to produce an iodine laser by energy transfer from the  $\text{O}_2(^1\Delta)$  to  $\text{I}_2$ . These experiments used a mixture of Ar at a partial pressure of 13.3 kPa and  $\text{O}_2$  at a partial pressure of 0.27 kPa; alpha particles from a  ${}^{10}\text{B}$  coating excited the mixture. Neutrons were provided by a TRIGA reactor, and steady-state as well as pulsed experiments were carried out. Results of these experiments indicate that  $\text{O}_2(^1\Delta)$  was produced in quantities in excess of those predicted from direct electron impact excitation. It was concluded that additional mechanisms such as recombination of atomic oxygen may have been a significant contributor to the  $\text{O}_2(^1\Delta)$  population under these conditions.

Walters et al. (ref. 66) carried out experiments to investigate the rare-gas halide lasers using a nuclear-pumped flash lamp. They studied, in detail, the production of  $\text{XeF}^*$  produced by the photolysis of  $\text{XeF}_2$  by  $\text{Xe}_2^*$  excimer emission. In these experiments, energy transfer efficiency from nuclear reaction to optical emission was measured to be  $67 \pm 20$  percent. The emission appeared in the  $\text{Xe}_2$  band centered at  $0.172 \mu\text{m}$ . No atomic emission lines were observed in the presence of the excimer fluorescence. Modeling of this system suggested that higher neutron fluxes might be successful in achieving lasing on the  $\text{XeF}^*(\text{C} \rightarrow \text{A})$  transition. An experimental laser and gain cell was constructed based on this model and tested in a fast-burst reactor. The data collected were limited and therefore inconclusive.

Lorents et al. (ref. 67) studied in detail the performance limits of fission-fragment-excited laser systems radiating in the near ultraviolet and visible regions. Their studies indicate that extremely high energy outputs appear feasible with pulsed reactors. They concluded that transverse dimensions of greater than 1 m were practical and that high-density gas phase media containing homogeneously integrated fissile material were superior to foil configurations. They also pointed out that the use of fissile materials with large fission cross sections, particularly in the epithermal range, increased the medium size and relaxed the kinetic and optical constraints. It was also shown that simulation of the conditions produced by fission fragment excitation could be achieved over most of the relevant parameter space by studies of candidate media using electron beams.

Dlabal et al. (ref. 68) investigated various atoms and molecules that appeared attractive as potential nuclear-pumped lasers. Much of their research was directed toward the study of the  $\text{IF}^*$  molecule. Using electron beam excitation, they identified the  $\text{IF}^*$  blue-green emission as the  $\text{E} \rightarrow \text{A}^3\Pi_1$  transition. A radiative lifetime of approximately 15 ns was determined for the upper state of the transition and the kinetic formation chain for  $\text{IF}^*$  was determined. These results suggested that  $\text{IF}^*$  was a very attractive candidate for a laser to be pumped by a gas core reactor, but no experiments were carried out in this area.

Experiments using the afterglow of an electrically pulsed laser were carried out by De Young et al. (ref. 40). These experiments showed the value of using the afterglow to study potential nuclear-pumped laser candidates. Systems that lased strongly in the afterglow consistently achieved lasing with direct nuclear pumping, because both the electrically pulsed afterglow and the nuclear-induced plasma were dominated by collisional-radiative recombination.

## CONCLUSION

In 1980, the program goals of the NASA nuclear-pumped laser program had been achieved in that a direct nuclear-pumped laser operating at the kilowatt power level had been demonstrated and the first steps toward a gas core laser-reactor using  $^{235}\text{UF}_6$  as fuel had been taken. All known nuclear-pumped lasers, as of 1981, are listed in the following table:

	Reaction	Wavelength, $\mu\text{m}$	Minimum lasing threshold, $\text{n/m}^2\text{-s}$	Peak laser output	
				Pressure, kPa	Power, W
NASA Langley:					
$^3\text{He-CO}$	$^3\text{He}(n,p)^3\text{H}$	5.00	$3 \times 10^{20}$	200	200
$^3\text{He-Ar}$		1.79, 1.27	$2.5 \times 10^{20}$	200	4
$^3\text{He-Ar}$		1.79	$1 \times 10^{20}$	300	1012
$^3\text{He-Cl}$		1.586	$7 \times 10^{19}$	80	0.1
$^3\text{He-Xe}$		3.508, 2.027, 3.652	$4 \times 10^{19}$	200	<10
$^3\text{He-Xe}$		2.63	$3 \times 10^{20}$	300	200
$^3\text{He-Kr}$		2.19, 2.52	$1 \times 10^{21}$	26.6	0.001
Ar-Xe	$^{235}\text{UF}_6(n,ff)\text{FF}$	2.65	$4 \times 10^{19}$	80	4.6
Sandia Labs.: CO	$^{235}\text{U}(n,ff)\text{FF}$	5.1-5.6	$5 \times 10^{20}$	13.3	100
Los Alamos and Univ. of Florida:					
$^4\text{He-Xe}$	$^{235}\text{U}(n,ff)\text{FF}$	3.51	$5 \times 10^{17}$	26.6	0.01
$^3\text{He-Xe}$	$^3\text{He}(n,p)^3\text{H}$	2.027, 3.5, 3.65	$3 \times 10^{20}$	77	0.5
$^3\text{He-Ne}$	$^3\text{He}(n,p)^3\text{H}$	0.6328	$2 \times 10^{15}$	40	0.00001
He-N <sub>2</sub> -CO <sub>2</sub>	Transfer	10.6		1.1, 0.53	100
Univ. of Illinois:					
Ne-N <sub>2</sub>	$^{10}\text{B}(n,\alpha)^7\text{Li}$	0.863, 0.939	$1 \times 10^{19}$	20	0.001
$^4\text{He-Hg}$		0.615	$1 \times 10^{20}$	80	0.001
$^4\text{He-CO}$		1.45	$4 \times 10^{18}$	6.7-80	
$^4\text{He-CO}_2$		1.45	$4 \times 10^{18}$	6.7-80	
Soviet Union:					
$^4\text{He-Ar}$	$^{235}\text{U}(n,ff)\text{FF}$	2.397, 1.19, 1.15	$1 \times 10^{20}$	200	30
$^4\text{He-Xe}$		2.63, 2.48	$1 \times 10^{19}$	400-500	2000
$^4\text{He-Kr}$		2.52	$1 \times 10^{19}$	100	10
$^3\text{He-Cd}$	$^3\text{He}(n,p)^3\text{H}$	0.5337, 0.5378	$3 \times 10^{18}$	53	0.1



Much more was accomplished in the nuclear-pumped laser program including

1. Techniques necessary to carry out high-quality laser research in the hostile environment of a nuclear reactor were mastered.
2. Basic understanding of the dominant processes occurring in nuclear-induced plasmas were identified.
3. Several mechanisms for producing population inversions in nuclear-induced plasmas were identified.
4. Scalability over a limited range of total gas pressure and neutron flux was established.

The research funded by NASA has brought this area of research out of its infancy and established a data base for nuclear-powered lasers. Considerable research remains to be done before a self-critical laser-reactor system becomes a reality. This research should particularly address the problems of finding laser systems which are compatible with  $^{235}\text{UF}_6$  and have high power outputs. Although these are difficult problems, they do not appear insurmountable. Rapid progress in nuclear-pumped lasers has been made, but their full potential is far from being realized.

Langley Research Center  
National Aeronautics and Space Administration  
Hampton, VA 23665  
November 4, 1982

## REFERENCES

1. Herwig, Lloyd O.: Summary of Preliminary Studies Concerning Nuclear-Pumping of Gas Laser Systems. Rep. C-110053-5, United Aircraft Corp., Feb. 1964.
2. DeShong, James A., Jr.: Optimum Design of High-Pressure, Large-Diameter, Direct-Nuclear-Pumped, Gas Lasers. ANL-7030 (Contract W-31-109-eng-38), Reactor Physics Div., Argonne National Lab., June 1965.
3. Rusk, J. R.; Cook, R. D.; Eerkens, J. W.; DeJuren, J. A.; and Davis, B. T.: Research on Direct Nuclear Pumping of Gas Lasers (DNPGL). Tech. Rept. AFAL-TR-68-256, U.S. Air Force, Dec. 1968. (Available from DTIC as AD 680 406.)
4. Derr, V. E.; McNice, G. T.; and Rushworth, P. M.: Application of Nuclear Radiation to the Pumping of Lasers. Radioisotopes for Aerospace - Part 2: Systems and Applications, John C. Dempsey and Paul Polishuk, eds., Plenum Press, Inc., 1966, pp. 309-346.
5. Russell, G. R.: Feasibility of a Nuclear Laser Excited by Fission Fragments Produced in a Pulsed Nuclear Reactor. Research on Uranium Plasmas and Their Technological Applications, Karlheinz Thom and Richard T. Schneider, eds., NASA SP-236, 1971, pp. 53-62.
6. Schneider, R. T.: On the Feasibility of Nuclear Pumping of Gas Lasers. Laser Interaction and Related Plasma Phenomena - Volume 3A, Helmut J. Schwarz and Heinrich Hora, eds., Plenum Press, Inc., c.1974, pp. 85-107.
7. Walters, R. A.: Excitation and Ionization of Gases by Fission Fragments - Application to Direct Nuclear Pumping and Gas Lasers. Ph. D. Thesis, Univ. of Florida, 1973.
8. Shipman, G. R.; Walters, R. A.; and Schneider, R. T.: Population Inversions in Fission Fragment Excited Helium. Trans. American Nucl. Soc., vol. 17, 1973, pp. 3-4.
9. Lo, Ronnie H.; and Miley, George H.: Electron Energy Distribution in a Helium Plasma Created by Nuclear Radiations. IEEE Trans. Plasma Sci., vol. PS-2, no. 4, Dec. 1974, pp. 198-205.
10. Hassan, H. A.; and Deese, Jerry E.: Electron Distribution Function in a Plasma Generated by Fission Fragments. Phys. Fluids, vol. 19, no. 12, Dec. 1976, pp. 2005-2011.
11. Guyot, J. C.; Miley, G. H.; and Verdeyen, J. T.: Application of a Two-Region Heavy Charged Particle Model to Noble-Gas Plasmas Induced by Nuclear Radiations. Nucl. Sci. & Eng., vol. 48, no. 4, Aug. 1972, pp. 373-386.
12. Deese, Jerry E.; and Hassan, H. A.: Analysis of Nuclear Induced Plasmas. AIAA J., vol. 14, no. 11, Nov. 1976, pp. 1589-1597.
13. Thiess, P. E.; and Miley, G. H.: Calculations of Ionization-Excitation Source Rates in Gaseous Media Irradiated by Fission Fragments and Alpha Particles. Research on Uranium Plasmas and Their Technological Applications, Karlheinz Thom and Richard T. Schneider, eds., NASA SP-236, 1971, pp. 369-396.

14. Hassan, H. A.: Analysis of an He-N<sub>2</sub>-CO<sub>2</sub>-UF<sub>6</sub> Laser System. AIAA J., vol. 19, no. 7, July 1981, pp. 893-898.
15. Wilson, J. W.; De Young, R. J.; and Harries, W. L.: Nuclear-Pumped <sup>3</sup>He-Ar Laser Modeling. J. Appl. Phys., vol. 50, no. 3, Mar. 1979, pp. 1226-1235.
16. Wilson, J. W.; and De Young, R. J.: Power Density in Direct Nuclear-Pumped <sup>3</sup>He Lasers. J. Appl. Phys., vol. 49, no. 3, Mar. 1978, pp. 980-988.
17. Wilson, John W.; and De Young, R. J.: Power Deposition in Volumetric <sup>235</sup>UF<sub>6</sub>-He Fission-Pumped Nuclear Lasers. J. Appl. Phys., vol. 49, no. 3, Mar. 1978, pp. 989-993.
18. Herwig, L. O.: Study of Nuclear-Radiation Pumping of Gas-Laser Systems. Bull. American Phys. Soc., ser. 11, vol. 9, no. 2, Feb. 27, 1964, p. 160.
19. Herwig, Lloyd O.: Concepts for Direct Conversion of Stored Nuclear Energy to Laser Beam Power. Trans. American Nucl. Soc., vol. 7, no. 1, June 1964, pp. 131-132.
20. Eerkens, J. W.; Cook, R. D.; and Rusk, J. R.: Research on Direct Nuclear Pumping of Gas Laser. Rept. NSL-66-141-1 (Contract AF 33-615-5000), Northrop Space Labs, Sept. 1966. (Available from DTIC as AD 807 472.)
21. Davis, B. I.; and DeJuren, J. A.: Nuclear-Pumped Noble-Gas Ion-Laser Experiments. NCL-68-13R, Northrop Corporate Labs.
22. Guyot, J. C.; Miley, G. H.; Verdeyen, J. T.; and Ganley, T.: On Gas Laser Pumping via Nuclear Radiations. Research on Uranium Plasmas and Their Technological Applications, Karlheinz Thom and Richard T. Schneider, eds., NASA SP-236, 1971, pp. 357-368.
23. Allario, F.; Schneider, R. T.; Lucht, R. A.; and Hess, R. V.: Enhancement of Laser Output by Nuclear Reactions. Research on Uranium Plasmas and Their Technological Applications, Karlheinz Thom and Richard T. Schneider, eds., NASA SP-236, 1971, pp. 397-400.
24. Andriakhin, V. M.; Velikhov, E. P.; Golubev, S. A.; Krasil'nikov, S. S.; Prokhorov, A. M.; Pis'mennyi, V. D.; and Rakhimov, A. T.: Increase of CO<sub>2</sub> Laser Power Under the Influence of a Beam of Fast Protons. Soviet Phys. - JETP Lett., vol. 8, no. 7, Oct. 5, 1968, pp. 214-216.
25. Compton, D. M. J.; and Cesena, R. A.: Radiation Effects on Lasers. GA-7274 (Contract NAS 12-32), General Atomic, Division of General Dynamics, Sept. 21, 1966. (Available as NASA CR-79108.)
26. Tittel, F.; and Kamel, N.: Radiation Effects in Glass Lasers. Interaction of Radiation With Solids, Adli Bishay, ed., Plenum Press, Inc., 1967, pp. 261-272.
27. McArthur, D. A.; and Tollefsrud, P. B.: Observation of Laser Action in CO Gas Excited Only by Fission Fragments. Appl. Phys. Lett., vol. 26, no. 4, Feb. 15, 1975, pp. 187-190.

28. Helmick, H. H.; Fuller, J. L.; and Schneider, R. T.: Direct Nuclear Pumping of a Helium-Xenon Laser. *Appl. Phys. Lett.*, vol. 26, no. 6, Mar. 15, 1975, pp. 327-328.
29. De Young, R. J.; Wells, W. E.; Miley, G. H.; and Verdeyen, J. T.: Direct Nuclear Pumping of a Ne-N<sub>2</sub> Laser. *Appl. Phys. Lett.*, vol. 28, no. 9, May 1, 1976, pp. 519-521.
30. Thom, K.; and Schneider, R. T.: Gaseous Fuel Reactor Research. *IEEE Trans. Plasma Sci.*, vol. PS-5, no. 4, Dec. 1977, pp. 259-272.
31. De Young, R. J.; Wells, W. E.; and Miley, G. H.: Optical Gain in a Neutron-Induced <sup>3</sup>He-Ne-O<sub>2</sub> Plasma. *Appl. Phys. Lett.*, vol. 28, no. 4, Feb. 15, 1976, pp. 194-197.
32. Jalufka, N. W.; De Young, R. J.; Hohl, F.; and Williams, M. D.: Nuclear-Pumped <sup>3</sup>He-Ar Laser Excited by the <sup>3</sup>He(n,p)<sup>3</sup>H Reaction. *Appl. Phys. Lett.*, vol. 29, no. 3, Aug. 1, 1976, pp. 188-190.
33. De Young, R. J.; Jalufka, N. W.; and Hohl, F.: Nuclear-Pumped Lasing of <sup>3</sup>He-Xe and <sup>3</sup>He-Kr. *Appl. Phys. Lett.*, vol. 30, no. 1, Jan. 1, 1977, pp. 19-21.
34. Jalufka, N. W.: Nuclear-Pumped Lasing of <sup>3</sup>He-Xe at 2.63 μm. *Appl. Phys. Lett.*, vol. 39, no. 7, Oct. 1, 1981, pp. 535-536.
35. Voinov, A. M.; Dovbysh, L. E.; Krivonosov, V. N.; Mel'nikov, S. P.; Podmoshenskii, I. V.; and Sinyanskii, A. A.: Low-Threshold Nuclear-Pumped Lasers Using Transitions of Atomic Xenon. *Soviet Phys. - Doklady*, vol. 24, no. 3, Mar. 1979, pp. 189-190.
36. Voinov, A. M.; Dovbysh, L. E.; Krivonosov, V. N.; Mel'nikov, S. P.; Kazakevich, A. T.; Podmoshenskii, I. V.; and Sinyanskii, A. A.: Nuclear-Pumped IR Lasers Using ArI, KrI, and XeI Transitions. *Soviet Phys. - Tech. Phys. Lett.*, vol. 5, no. 4, Apr. 1979, pp. 171-172.
37. Newman, L. A.; and DeTemple, T. A.: High-Pressure Infrared Ar-Xe Laser System: Ionizer-Sustainer Mode of Excitation. *Appl. Phys. Lett.*, vol. 27, no. 12, Dec. 15, 1975, pp. 678-680.
38. Mansfield, C. R.; Bird, P. F.; Davis, J. F.; Wimett, T. F.; and Helmick, H. H.: Direct Nuclear Pumping of a <sup>3</sup>He-Xe Laser. *Appl. Phys. Lett.*, vol. 30, no. 12, June 15, 1977, pp. 640-641.
39. Carter, B. D.; Rowe, M. J.; and Schneider, R. T.: Nuclear-Pumped cw Lasing of the <sup>3</sup>He-Ne System. *Appl. Phys. Lett.*, vol. 36, no. 2, Jan. 15, 1980, pp. 115-117.
40. De Young, R. J.; Jalufka, N. W.; and Hohl, F.: Direct Nuclear-Pumped Lasers Using the <sup>3</sup>He(n,p)<sup>3</sup>H Reaction. *AIAA J.*, vol. 16, no. 9, Sept. 1978, pp. 991-998.
41. Jalufka, N. W.; and Hohl, F.: A Direct Nuclear-Pumped <sup>3</sup>He-CO Laser. *Appl. Phys. Lett.*, vol. 39, no. 2, July 15, 1981, pp. 139-142.

42. De Young, Russell J.; and Hohl, Frank: Large Volume Multiple Path Nuclear Lasing of  $^3\text{He-Ar}$ . IEEE J. Quantum Electron., vol. QE-16, no. 10, Oct. 1980, pp. 1114-1117.
43. De Young, R. J.: Kilowatt Multiple-Path  $^3\text{He-Ar}$  Nuclear-Pumped Laser. Appl. Phys. Lett., vol. 38, no. 5, Mar. 1, 1981, pp. 297-298.
44. Jalufka, N. W.: Direct Nuclear-Pumped Laser Amplifier. Appl. Phys. Lett., vol. 39, no. 9, Nov. 1, 1981, pp. 690-692.
45. Batyrbekov, G. A.; Danilychev, V. A.; Kovsh, I. B.; Mardenov, M. P.; and Khasenov, M. V.: Preionization  $\text{CO}_2$  Laser Operating in the Active Zone of a Stationary Nuclear Reactor. Sov. J. Quantum Electron., vol. 7, no. 5, May 1977, pp. 667-668.
46. Batyrbekov, G. A.; Danilychev, A. A.; Ionin, A. A.; Kovsh, I. B.; Kunakov, S. K.; Mardenov, M. P.; and Khasenov, M. V.: Excitation of  $\text{CO} + \text{N}_2 + ^3\text{He}$  and  $\text{CO}_2 + \text{N}_2 + ^3\text{He}$  Laser Mixtures in an Externally Maintained Discharge in a Reactor Core. Izv. Akad. Nauk SSSR, Ser. Fiz., vol. 42, no. 12, 1978, pp. 2484-2487.
47. McArthur, D. A.; Miller, G. H.; and Tollefsrud, P. B.: Pumping of High-Pressure  $\text{CO}_2$  Laser Media via a Fast-Burst Reactor and Electrical Sustainer. Appl. Phys. Lett., vol. 23, no. 6, Sept. 15, 1973, pp. 303-305.
48. Jalufka, N. W.: Direct Nuclear Excitation of a  $^3\text{He-CO}_2$  Gas Mixture. Appl. Phys. Lett., vol. 39, no. 3, Aug. 1, 1981, pp. 190-192.
49. Mis'kevich, A. I.; Dmitriev, A. B.; II'yashchenko, V. S.; Salamakha, B. S.; Stepanov, V. A.; and Gorodkov, E. M.: Lasing in Cd Vapor Pumped by Products of the Nuclear Reaction  $\text{He}^3(n,p)\text{T}$ . Soviet Phys. - Tech. Phys. Lett., vol. 6, no. 7, July 1980, pp. 352-353.
50. McArthur, D. A.: Development of a Higher Power Fission-Fragment-Excited CO Laser. Proceedings of the Princeton University Conference on Partially Ionized Plasmas Including the Third Symposium on Uranium Plasmas, M. Krishnan, ed., NASA CR-157047, 1976, pp. 115-122.
51. Cooper, G. W.; and Verdeyen, J. T.: Recombination-Pumped Atomic Nitrogen and Carbon Afterglow Lasers. J. Appl. Phys., vol. 48, no. 3, Mar. 1977, pp. 1170-1175.
52. Akerman, M. A.; Miley, G. H.; and McArthur, D. A.: A Helium-Mercury Direct Nuclear Pumped Laser. Appl. Phys. Lett., vol. 30, no. 8, Apr. 15, 1977, pp. 409-412.
53. Andriakhin, V. M.; Vasil'nov, V. V.; Krasil'nikov, S. S.; Pis'mennyi, V. D.; and Khvostionov, V. E.: Radiation of  $\text{Hg-He}^3$  Gas Mixture Bombarded by a Neutron Stream. Soviet Phys. - JETP Lett., vol. 12, no. 2, July 20, 1970, pp. 58-59.
54. Prelas, M. A.; Akerman, M. A.; Boody, F. P.; and Miley, G. H.: A Direct Nuclear Pumped 1.45- $\mu$  Atomic Carbon Laser in Mixtures of  $\text{He-CO}$  and  $\text{He-CO}_2$ . Appl. Phys. Lett., vol. 31, no. 7, Oct. 1, 1977, pp. 428-430.

55. De Young, R. J.: Multiple-Path Fission-Foil Nuclear Lasing of Ar-Xe. Appl. Phys. Lett., vol. 39, no. 8, Oct. 15, 1981, pp. 585-587.
56. Miley, George H.: Some Unique Aspects of Recent Nuclear-Pumped Lasers Developed at the University of Illinois. First International Symposium on Nuclear Induced Plasmas and Nuclear Pumped Lasers, Les Editions de Physique (Orsay, France), 1978, pp. 87-102.
57. Rowe, M. J.; Liang, R. H.; and Schneider, R. T.: Nuclear Pumped CO<sub>2</sub>-Laser. 1981 IEEE International Conference on Plasma Science, c.1981, pp. 149-150.
58. De Young, R. J.; Shiu, Y. J.; and Williams, M. D.: Fission-Fragment Nuclear Lasing of Ar(He)-Xe. Appl. Phys. Lett., vol. 37, no. 8, Oct. 15, 1980, pp. 679-681.
59. Rodgers, Richard J.: Initial Conceptual Design Study of Self-Critical Nuclear Pumped Laser Systems. NASA CR-3128, 1979.
60. Miley, G. H.: Direct Nuclear Pumped Lasers - Status and Potential Applications. Laser Interaction and Related Plasma Phenomena - Volume 4A, Helmut J. Schwarz and Heinrich Hora, eds., Plenum Press, c.1977, pp. 181-228.
61. Fisher, Edward R.; and Lim, Soon S.: Modeling of DNP Laser Systems. RIES 79-130 (Contract No. DASG60-78-C-0055), Research Inst. for Eng. Sciences, Wayne State Univ., Mar. 1979.
62. Davis, John Franklin, III: Kinetic and Experimental Study of Argon and Argon-Nitrogen Mixtures Excited by Fission Fragments. Ph. D. Thesis, Univ. of Florida, 1976.
63. Zapata-Casares, Luis Enrique: The Kinetics of Fission Fragment Excited XeF\*. Ph. D. Diss., Univ. of Florida, 1981.
64. De Young, R. J.; and Weaver, W. R.: Spectra From Nuclear-Excited Plasmas. J. Opt. Soc. America, vol. 70, no. 5, May 1980, pp. 500-506.
65. Zediker, M. S.; Dooling, T. R.; and Miley, G. H.: A Potential Nuclear Pumped O<sub>2</sub>(<sup>1</sup>Δ)-I<sub>2</sub> Laser. 1981 IEEE International Conference on Plasma Science, c.1981, pp. 150-151.
66. Walters, R. A.; Cox, J. D.; Schneider, R. T.; and Hagefstration, J.: Generation, Measurement, and Utilization of Xenon Excimer Radiation Produced by Nuclear Reaction Products. Trans. American Nucl. Soc., vol. 34, 1980, pp. 808-810.
67. Lorents, D. C.; McCusker, M. V.; and Rhodes, C. K.: Nuclear Fission Fragment Excitation of Electronic Transition Laser Media. Proceedings of the Princeton University Conference on Partially Ionized Plasmas Including the Third Symposium on Uranium Plasmas, M. Krishnan, ed., NASA CR-157047, 1976, pp. 109-114.
68. Dlabal, M. L.; Hutchinson, S. B.; Eden, J. G.; and Verdeyen, J. T.: Multiline (480-496 nm) Discharge-Pumped Iodine Monofluoride Laser. Appl. Phys. Lett., vol. 37, no. 10, Nov. 15, 1980, pp. 873-876.



1. Report No. NASA TP-2091		2. Government Accession No.		3. Recipient's Catalog No.	
4. Title and Subtitle  DIRECT NUCLEAR-PUMPED LASERS				5. Report Date January 1983	
				6. Performing Organization Code 506-55-13-01	
7. Author(s)  N. W. Jalufka				8. Performing Organization Report No. L-15168	
9. Performing Organization Name and Address  NASA Langley Research Center Hampton, VA 23665				10. Work Unit No.	
				11. Contract or Grant No.	
12. Sponsoring Agency Name and Address  National Aeronautics and Space Administration Washington, DC 20546				13. Type of Report and Period Covered Technical Paper	
				14. Sponsoring Agency Code	
15. Supplementary Notes					
16. Abstract  <p>The development of direct nuclear-pumped lasers is reviewed from the earliest known studies to the present. Theoretical and experimental investigations of various methods of converting the energy of nuclear fission fragments to laser power are summarized. After initial successes in the mid-1970's, the development of direct nuclear-pumped lasers proceeded rapidly and several nuclear-pumped lasers were achieved. Much of the research in this area did not produce a direct nuclear-pumped laser, but this was not always the intent, since the research was done in order to understand the basic processes involved in the production of a plasma by nuclear radiation. Significant progress was accomplished in this area and a large amount of basic data on plasma formation and atomic and molecular processes leading to population inversions is now available.</p>					
17. Key Words (Suggested by Author(s))  Lasers Nuclear pumping Energy conversion Recombination lasers Nuclear-induced plasmas			18. Distribution Statement  Unclassified - Unlimited   Subject Category 36		
19. Security Classif. (of this report) Unclassified	20. Security Classif. (of this page) Unclassified	21. No. of Pages 52	22. Price* A04		